Investigation of Limiter Recycling in the Divertor Tokamak ASDEX

F. Wagner

IPP III/71 August 1981

MAX-PLANCK-INSTITUT FÜR PLASMAPHYSIK

8046 GARCHING BEI MÜNCHEN

MAX-PLANCK-INSTITUT FÜR PLASMAPHYSIK

GARCHING BEI MÜNCHEN

Investigation of Limiter Recycling in the Divertor Tokamak ASDEX

F. Wagner

IPP III/71 August 1981

Die nachstehende Arbeit wurde im Rahmen des Vertrages zwischen dem Max-Planck-Institut für Plasmaphysik und der Europäischen Atomgemeinschaft über die Zusammenarbeit auf dem Gebiete der Plasmaphysik durchgeführt.

IPP III/71 F. Wagner

Investigation of Limiter Recycling in the Divertor Tokamak ASDEX

August 1981

Abstract

A divertor experiment like the ASDEX tokamak is especially suited for studying ion recycling at a material limiter, because the plasma can alternatively be limited by a magnetic limiter (separatrix) or by a material limiter. The role of the material limiter in ion recycling is documented by observing the increase in charge exchange flux emitted at the limiter position, and the decrease in external gas input necessary to keep the plasma line density invariant, when the material limiter is moved to the plasma. Ion recycling occurs predominantly at the outside section of a ring limiter. The limiter material saturates shortly after the start of the discharge. About 6o % of the total recycling occurs at the limiter, which is nearly 1oo % of the ion recycling. The remaining 4o % of the total recycling is carried by charge exchange neutrals. Due to saturation, the recycling coefficient at the limiter is 1; the recycling coefficient of the charge exchange neutrals at the wall is approximately 0.5 giving rise to a total recycling coefficent of limiter discharges of 0.8 - 0.9. It is observed that the plasma resistivity increases when the material limiter is moved toward the separatrix. The increase in Z_{eff} can tentatively be explained by proton sputtering.

1. Introduction

Recycling denotes the circular process whereby plasma particles (ions and neutrals), which leave the plasma and hit the wall, are reemitted from the wall and subsequently re-ionized within the plasma /1,2/. Plasma particles are lost by the formation of charge exchange neutrals and by diffusion of charged particles across the magnetic field. At a given external particle input recycling and magnetic confinement determine the plasma content. Without recycling the plasma content would decay within the global particle confinement time τ_p after the external gas flux has been turned off. Recycling increases the decay time of the plasma particle content to the value $\tau_{eff} = \tau_p/(1-r)$; r is the recycling coefficient. τ_p and r are values averaged over ions and neutrals.

Recycling during a tokamak discharge has to be studied in detail to find means to control recycling so that the plasma density is a quantity which can be set and controlled by the external gas feed. This is particularly important with auxiliary heating, especially neutral injection, as here the heating is based on the injection of additional particles.

Another motivation to study recycling and to find the location where it predominantly occurs is that the processes which give rise to recycling also cause the release of impurities from the wall.

The divertor tokamak ASDEX is especially suited to investigate recycling because the plasma can alternatively be limited by a magnetic limiter (separatrix) or by a material limiter. Thus recycling of divertor (D) discharges or of limiter (L) discharges respectively,can separately be studied.

In this work we report on recycling studies with discharges limited by a material limiter. Recycling studies of divertor discharges of ASDEX are summarized in /3/.

2. Experimental Details

ASDEX is a large divertor tokamak. The main parameters of ASDEX are summarized in Table 1. Details of the machine are given in /4,5/. A special feature of ASDEX is the pair of coil-triplets located at top and bottom sides of the plasma which give rise to a separatrix and a poloidal divertor configuration. With the coil triplets activated the plasma is limited by the separatrix.

Alternatively, ASDEX can be run as a classical tokamak with a material limiter. Due to the triplet configuration of the divertor coils, and to correction coils located outside of the vacuum vessel, a divertor plasma with circular cross-section is achieved which allows close comparison with the material limiter discharges. In particular, this configuration allows a detailed study of the plasma-limiter interaction, because the material limiter can be moved in steps toward the plasma surface while the plasma is limited by the magnetic limiter. The position of the magnetic axis, plasma shape and minor axis do not change during the transition from divertor to limiter configuration. Programmable feedback systems keep the time variation of plasma current, electron line density, vertical and radial position constant.

Two types of material limiters are used. A stainless steel ring limiter formed by two half sectors which can individually be rotated in steps by a pneumatic system from outside during the periods between discharges. Thereby, recycling at the outside limiter can be studied separately from the recycling at the inside limiter.

In Fig.1 the cross-sections for the two plasma configurations are shown; case (a) shows the divertor configuration with the separatrix and case (b) shows the limiter configuration with the two limiter wings.

In addition to the circular limiter a mushroom limiter is installed in the mid-plane of the plasma. The mushroom limiter can be moved in steps and between discharges toward the plasma separatrix. Three different materials for the mushroom limiter have been tested: A cylindrical stainless-steel limiter, a cylindrical graphit-limiter each with a diameter of 14 cm and a SiC-limiter formed by 5 individual SiC knobs each with a diameter of 3.8 cm /6/.

Recycling is studied with 2 charge exchange analyzers, a 5 channel analyzer NEA5 positioned at the location of the ring limiter and a 1o channel analyzer NEA1o positioned 45° from the limiter position. NEA5 can be rotated in the toroidal direction while NEA1o can be rotated in a ploidal plane.

Figure 2 shows the toroidal positions of the two types of limiters, the calibrated gas input and the location of the dignostic equipment.

3. Hydrogen Recycling at the Material Limiter

3.1 Charge Exchange Measurements at the Limiter

Figure 3 shows a toroidal section of the plasma with the two ring limiter wings. The distance from the limiter to the separatrix is denoted Δr.

Figure 4 shows the charge exchange spectra measured near the limiter (NEA5) during several identical feedback controlled plasma shots with different distances Δr of the outside limiter

wing from the separatrix. The charge exchange flux is measured perpendicular to the plasma surface. The line of sight of the analyzer is 11 cm away from the plane of the limiter hinges.

When the limiter approaches the plasma surface the charge exchange flux close to the limiter increases because the neutral gas density at the limiter increases. The increase in neutral gas density is caused by the neutralization of toroidally circulating protons at the limiter. More ions are neutralized when the limiter is moved toward the plasma because the proton density in the boundary layer increases toward the separatrix. It is interesting to note that without a limiter the proton density reaches to the wall, so that any remote obstacle can enhance the local recylcing. Figure 5 shows the time variation of the charge exchange flux at E = 75o eV at limiter distances between 4 cm and 11 cm from the separatrix. The flux increases already by about 5o % when the limiter is moved from 11 cm from the separatrix to 8 cm. Figure 6 shows the variation of the normalized charge exchange flux at 2 keV again as a function of limiter-separatrix distance Δr for two cases: First measured close to the limiter with the analyzer NEA5 and second measured far from the limiter with NEA10 looking at the plasma center. Contrary to the increase of charge exchange flux at the limiter, the charge exchange flux away from the limiter decreases.

One possibility is that the limiter blocks the drift of the ions to the wall so that ion recycling at the wall is reduced in favor of enhanced limiter recycling. Another and more reasonable possibility for the observed reduction in wall recycling is that the material limiter interrupts the flow of ions into the divertor and the subsequent backflow of hydrogen gas into the main plasma chamber which otherwise could give rise to enhanced charge exchange flux at a position far from the limiter.

We have studied the toroidal extent of the increase of neutral gas density at the limiter by rotating the charge exchange analyzer NEA5 in the toroidal direction. The geometry for these investigations is shown in Fig. 7. The charge exchange flux spectra measured at different toroidal distances from the limiter are plotted in Fig.8. Curve 1 and 2 are obtained with NEA5, curve 3 is measured by NEA1o. With the absolute values of the flux spectra shown in Fig.8 and the Monte Carlo code AURORA /7/ we have calculated the neutral density profiles within poloidal planes with different toroidal distances $R\Delta\varphi$ from the limiter plane (see Fig.9). Within the limiter plane we observe a neutral density of nearly $1o^{11}$ (atoms/cm^3) at the separatrix which falls off to about $1o^9$ (atoms/cm^3) toroidally away from the limiter. The absolute values are only qualitative because first the charge exchange flux is not measured in a strict poloidal plane for all cases when the analyzer is moved toroidally, and second the calculation of neutral density is carried out with a 1-dimensional code which assumes homogenity of the plasma properties in the poloidal and toroidal directions. The actual decrease of the neutral density away from the limiter may be sharper than measured here.

In order to estimate the total increase of hydrogen atoms within the plasma caused by the recycling at the limiter, the neutral density profiles shown in Fig.9 are integrated to give the areal density within a poloidal plane. The result of the integration is plotted in Fig.1o. The neutral density decreases with the distance from the limiter within a characteristic length of 43 cm. In reality the conditions are somewhat too involved to be characterized by one decay-length. Figure 11 shows the normalized charge exchange flux for different particle energies again plotted versus the toroidal distance from the limiter plane. It is observed that the decay length increases with the particle energy. The higher the energy of the particles the deeper is their origin within the plasma and the more spread out is the neutral gas density from the limiter due to charge exchange pro-

cesses in the bulk of the plasma. At the plasma edge the decay length of the neutral density is shorter than in the plasma center. The decrease of the neutral density far within the plasma cannot be approximated by an exponential variation. Preliminary calculations with a 2-dimensional neutral transport code indicate that the characteristic decay length depends on the distance between plasma and wall /8/. The actual value of 4o cm may be influenced by a large tank which is mounted to the vacuum vessel at the position of the limiter (see Fig.2).

We have used the exponential variation of the areal density as plotted in Fig. 1o and calculated the overall increase in neutral particle number within the torus caused by the recycling at the limiter. The enhancement is approximately a factor 4 - 5 over the case with no limiter.

3.2 Measurement of External Gas Flux into the Discharge

The plasma discharges with variable limiter positions from shot to shot are carried out at a fixed plasma density which is controlled by a programmable feedback system. With the assumption that the particle confinement time does not change with the limiter position, one expects that the plasma source, which is by ionization of neutrals, does not change as long as the plasma density does not change. From this consideration a neutral particle content within the plasma is expected independent of the limiter position. Consequently, the external gas input $\dot{Q}_G$ has to be decreased in a way that compensates for the increase of neutral density at the limiter due to recycling.

Figure 12a shows the external gas input during a plasma discharge necessary to produce the plotted line density (dashed curve) for different ring limiter distances from the separatrix. Figure 12b shows the same quantitiy for a stainless steel mushroom limiter.

(The external gas valve is switched off at .7 sec so that the electron density decays consecutively). The external gas input decreases as soon as the recycling at the limiter contributes to the effective particle confinement within the plasma. During the density plateau phase the necessary external gas input is about a factor 3.5 lower when the limiter is at the separatrix, than it is for a divertor discharge with the limiter 4 cm away. There is fair agreement between the factor 3.5 from the external gas flow and the factor 4 - 5 obtained by volume integrating the neutral density.

3.3 Saturation Effects at the Limiter

During the initial phase of the plasma discharge, when the density is still being built-up, the time variation of the external gas flow depends on the position of the limiter. This is clearly observed in Figs.12a and b for the SS-ring limiter and a SS-mushroom limiter.

At a limiter distance 3 - 4 cm away from the separatrix the required gas input into the discharge increases during the density rise. At the limiter position ($\Delta r = 0$), however, the gas input has a maximum (arrow in Fig.12a) and begins to decrease before the plasma density reaches its maximum (plateau) value. From the limiter position $\Delta r = 0$ to $\Delta r = 4$ the slope of the $\dot{Q}_G$ curve gradually changes.

This dependence on the limiter position of the necessary amount of external gas clearly indicates that the contribution of recycling at the limiter increases with the approach of the limiter toward the plasma and the decrease in $\dot{Q}_G$ for $\Delta r = 0$ points out that the recycling coefficient of the limiter increases and reaches 1 already during the initial phase of the discharge. With the assumption that the saturation fluence of stainless steel is 2×10^{18} protons/cm^2 /9/ it is easy to show that the limiter material saturates after about 0.3 sec for the conditions shown in Fig.12.

We have tried to model the saturation effects at the limiter by assuming that the recycling coefficient at the limiter increases linearly with the fluence to the limiter and stays at 1 after the saturation fluence of 2×10^{18} protons/cm^2 is reached. The necessary external gas flux to produce a linearly increasing density (dashed line in Fig. 13) is calculated from the particle balance equation assuming a particle confinement time of 35 msec. The external gas flux necessary for a stationary plasma with a line averaged density of 2×10^{13} cm^{-3} is estimated to be 2×10^{21} atoms/sec (see Section 3.5) without any limiter recycling. Figure 13 shows the result of the calculation, with $\emptyset_s = 2 \times 10^{18}$ protons/sec as saturation fluence, to produce the linearly rising density (dashed curve) for three different limiter positions. For the density decay length in the boundary layer a measured value of 2.5 cm is used. A comparison with Fig.12a documents that the salient features of the time variation of the external gas input are reproduced.

The saturation of the limiter material very early in the discharge can also be observed by the outgassing of the limiter as soon as the external gas flux into the discharge is terminated. Figure 14 compares the variation of the line averaged density $\bar{n}$ and the charge exchange flux $\dot{N}$ measured at the limiter position of a divertor (D) and a limiter (L) discharge. In a divertor discharge, the density decreases after the gas valve is switched off, with a discontinuity in the slope of the density curve. There is no such discontinuity in the case of the limiter discharge. The variation of the charge exchange flux $\dot{N}$ with and without limiter is similar to the corresponding variation of the density for the two cases.

Outgassing effects are particularly observed with the use of a graphite mushroom limiter as shown in Fig. 15. With the limiter moved to the plasma ($\Delta r = 0$), the external gas input necessary to

keep the density constant nearly vanishes. From comparison with other mushroom limiters, an outgassing rate of approximately 2.5×10^{-2} mbl/sec^{-1}cm^{-2} can be estimated. Because use of the carbon limiter increases the plasma resistivity, it is assumed that most of the outgassing is of impurities (see Chapter 4) rather than hydrogen.

3.4 Inside-outside Asymmetry in Limiter Recycling

It has been documented, that the charge exchange flux increases when the outside limiter wing is moved toward the plasma. Figure 16 compares the different recycling efficiencies of outside- and inside limiter wings again documented by the resulting increase in charge exchange flux when the limiter wing is moved to the plasma. Plotted is the flux at 5oo eV particle energy, but the wide discrepancy between inside and outside limiter segments is observed for all measured particle energies up to several keV. These particles emerge from the plasma center at an intensity which should not show much poloidal asymmetry due to absorption effects within the plasma.

Figure 17a shows charge exchange flux spectra measured with both limiter wings moved to the wall (circles) and spectra measured with the inside limiter wing rotated to the plasma (dots). It again indicates the lack of recycling at the inside limiter. These flux measurements are carried out with a well centered plasma without any vertical shift, which results in a so-called double null divertor configuration (see inset to Fig. 17a). The existence of a double null divertor configuration depends critically on the vertical positioning and can easily be monitored by the line density values measured in the upper and lower divertor chambers. The flux spectra plotted in Fig. 17b are measured for a plasma which is shifted vertically by 3 cm. A

single null divertor plasma is obtained (see inset to Fig.17b) and there is a very low plasma density in the lower divertor chamber. In this configuration, the rotation of the inside limiter to the plasma causes a slight increase in charge exchange flux.

These experimental results can be summarized as follows: Recycling occurs predominantly at the plasma outside (possibly because of a corresponding radial transport). If the inside boundary and the outside boundary of a divertor plasma are connected (by shifting the plasma in vertical direction) then part of the ion flux is directed to the inside boundary and can then recycle at the inside limiter.

An inside-outside asymmetry is also observed in the electron line densities of the inside and outside boundary layers in the divertor, and the power fluxes to the inside and outside neutralizer plates, respectively /5/.

3.5 Analysis of the Particle Balance Equation

We have shown that the effective particle confinement of limiter discharges is governed by recycling which predominantly occurs at the limiter and partly at the wall. The time variation of the total particle content N is described by eq. (1).

$$\frac{dN}{dt} + \frac{N}{\tau_p} = \dot{Q}_L + \dot{Q}_W + \dot{Q}_G \qquad (1)$$

$\dot{Q}_L$ is the recycling flux emerging from the limiter:

$$\dot{Q}_L = f_L r_L \frac{N}{\tau_p} \qquad (2)$$

f_L is the fraction of the plasma loss which recycles at the limiter; we have seen that the recycling coefficient $r_L=1$ due to saturation.

$\dot{Q}_W$ is the recycling flux from the wall:

$$\dot{Q}_W = (1-f_L) r_w \frac{N}{\tau_p} \tag{3}$$

$\dot{Q}_G$ is the external gas input.

That the recycling flux from the limiter and the external gas input are additive is seen in Fig.18. Plotted is the external gas flux $\dot{Q}_G$ versus the charge exchange flux Ø emitted at the limiter. Ø represents a variable which is proportional to the recycling flux at the limiter. $\dot{Q}_G$ and Ø of Fig. 18 are simultaneously varied by changing the distance Δr between separatrix and outside ring limiter wing. A linear relationship between $\dot{Q}_G$ and Ø is observed as expected from eq.(1), for stationary conditions and Q_W = const.. Without limiter recycling the necessary external gas flux, obtained by extrapolation to the ordinate, is 2×10^{21} atoms/sec. With limiter, the external gas flux decreases to about 5×10^{20} atoms/sec.

It is not a gratifying task to deduce recycling coefficients and assign numbers to the different fluxes of eq.(1) because numbers comparable in size have to be subtracted, so that the accuracy of the calculated coefficients relies heavily on the error bars of the measured quantities. In addition, the global values depend on quantities which have to be volume integrated and thereby appreciable errors can be introduced by a lack of precise knowledge of the poloidal and toroidal variation of the underlying source terms. Therefore, the following figures can only be regarded as rough estimates.

The plasma loss term N/τ_p is calculated from the line average density $\bar{n}$, the assumption of parabolic density profile and a particle confinement time $\tau_p = 35$ msec at $\bar{n} = 2.1 \times 10^{13} cm^{-3}$. τ_p is deduced from density decay experiments of heavily gettered (DP)

divertor discharges. By this means, the recycling of ions is nearly prevented so that the shortest density decay time of 4o msec represents the inherent particle confinement time. $\tau_p = 35$ msec is obtained after considering the still present recycling of neutrals. A similar value for τ_p is deduced from the variation of the plasma density with external gas input in DP discharges. For comparison, the energy confinement time is also approximately 35 msec in these discharges.

From the necessary gas inflow with and without limiter, and from the measured backflow of gas-out of the divertor chambers, the recycling flux at the limiter can be estimated:

$$\dot{Q}_L \sim 1.5 \times 1o^{21} \text{ atoms/sec.}$$

From eq.(2) f_L is deduced assuming $r_L = 1$.

$$f_L = 0.6o.$$

6o % of the plasma loss is compensated by recycling at the limiter. The rest is compensated by wall recycling and external gas input.

$$\dot{Q}_W = (1-f_L) r_W \frac{N}{W\tau_p} \simeq 5 \times 1o^{2o} \text{ atoms/sec}$$

from which a wall recycling coefficient of about 0.5 is deduced. The charge exchange loss at a location far away from the limiter is approximately $1.6 \times 1o^{15}$ atoms/cm^{2}sec which gives $4 - 5 \times 1o^{2o}$ atoms/sec totally. The comparison with $\dot{Q}_W$ shows that most of the wall recycling can be carried by charge exchange neutrals and that ion recycling at the wall or at other obstacles apart from the limiter is obviously of no major importance. This conclusion is also drawn from collecting carbon probe measurements. Only about 4 % of the ions which leave the plasma boundary reach the wall /1o/.

The global recycling coefficient of a limiter discharge is obtained by adding the weighted contribution from limiter and wall.

$$r = f_L r_L + (1-f_L) r_w = 0.8 - 0.9.$$

The global recycling coefficient r obtained by analyzing the different hydrogen fluxes during the stationary discharge phase can be compared with r deduced from the density decay time τ_{eff} after switching off the external gas valve.

$$\tau_{eff} = \tau_p/(1-r)$$

τ_{eff} for limiter discharges are typically 4oo msec yielding $r = 0.9$.

4. The Limiter as a Source of Impurities

The microscopic surface effects - reflection and desorption - which give rise to recycling at the limiter can also cause the release of impurities from the limiter. Figure 19 shows the variation of ohmic heating power P_{OH}, the electron temperature T_e and the ion temperature T_i with the distance Δr of the limiter from the separatrix, for constant plasma current. In Fig.19a the results from variing the position of the outside wing of the stainless steel ring limiter, in Fig. 19b the results from the SiC-mushroom limiter and in Fig. 19c those from the carbon-mushroom limiter are plotted.

From the increase in the ohmic heating power and the increase in temperature an increase in Z_{eff} can be estimated. The increase in Z_{eff} in case of the SS-limiter is 5o %, in case of the SiC-limiter 5o % and in case of the carbon limiter 115%.

Figure 2o shows the variation of ion temperature with Δr observed for the SS-ring limiter at different moments during the discharge. The increase in temperature from a D to a L type discharge is observed throughout the discharge, which points toward a continuous erosion process at the limiter and may exclude arcing which is known to occur at the beginning and the end of a discharge.

Assuming proton sputtering at the limiter as the responsible impurity production mechanism, the iron density in the plasma can be calculated from the plasma outflux N_e/τ_p and the sputtering coefficient γ:

$$\phi_{Fe} = \gamma \frac{N_e}{\tau_p}$$

ϕ_{Fe} causes an iron density n_{Fe} within the plasma /11/.

$$n_{Fe} = \gamma \frac{N_e}{\tau_p} \frac{\Delta_{ion}}{D \cdot F}$$

Δ_{ion} is the ionization length of an iron atom at the plasma boundary, D is the iron diffusion coefficient and F is the plasma surface. With $\Delta_{ion} = 0.4$ cm, $D = 4000\ cm^2 sec^{-1}$ as deduced from experiment /5/ and $\gamma = 2.5 \times 10^{-3}$ /12/ as obtained at an edge ion temperature of 8o eV:

$$\frac{n_{Fe}}{n_e} \sim 10^{-4}.$$

This value is in good agreement with the spectroscopically measured iron concentration in limiter discharges /13/.

Though there is good agreement between estimated iron concentration from hydrogen sputtering at the limiter and measured iron concentration, the observed increase in Z_{eff} cannot be explained. For $\Delta Z_{eff} \sim 50$ % an iron concentration of 2×10^{-3} is required assuming that the abundant iron species is Fe^{16+}.

5. Summary

The main purpose of this report is to collect evidence for the role of the limiter in recycling the outward diffusing plasma ions. It has been shown that the divertor experiment ASDEX is particularly suited for such an investigation.

Apart from demonstrating the importance of limiter recycling, we have tentatively tried to apply a simple recycling model to the experimental findings. We conclude that about 6o % of the recycling occurs at the limiter, which comprises nearly 1oo % of the ion recycling. 4o % of the recycling may be carried by charge exchange neutrals to the walls. The recycling coefficient of ions at the limiter is close to 1 because of hydrogen saturation of the limiter material; the recycling coefficient of the charge exchange neutrals is about 0.5. The total recycling coefficient of limiter discharges is thus 0.8 - 0.9.

We have further shown that recycling at the limiter causes the release of impurities. From comparison with spectroscopic data there is evidence that proton sputtering at the limiter is a dominant erosion process.

Acknowledgement

Contributions and assistance of the ASDEX team particularly of W.Engelhardt, H.M.Mayer and G.Vlases and technical assistance by G. Zangl and G. Zimmermann are acknowledged.

References

/1/ E.S.Marmar, J. Nucl. Mat., 76&77 (1978) 59.

/2/ H.C.Howe, J. Nucl. Mat., 93&94 (198o) 17.

/3/ Proc. IAEA Techn. Committee Meeting on Divertors and Impurity Control, Garching 1981, IPP-Report III/73.

/4/ Technical details are given in: R.Allgeyer et al., Proc. 6th Symp. on Engin. Probl. of Fusion Research (New York, IEEE Nuclear and Plasma Sciences Society, 1976), p. 378.

/5/ Experimental results are given in: M.Keilhacker et al., Proc.8th Int. Conf. on Plasma Physics and Controlled Nuclear Fusion Research, Brussels 198o, IAEA-CN-38/O-1.

/6/ The Sic-knobs are envisaged for the Zephyr toroidal limiter. Details see: H.Kotzlowski, F.Mast and H.Vernickel, J. Nucl. Mat. 93&94 (198o) 442.

/7/ H.M.Hughes, D.E.Post, J. of Comp. Phys. 28 (1978) 43.

/8/ D.Reiter, private communication.

/9/ K.L.Wilson, G.T.Thomas and W.Bauer, Nucl.Technol. 29 (1976) 322.

/1o/ J.Roth, private communication.

/11/ W.Engelhardt and W.Feneberg, J. Nucl. Mat., 76&77 (1978) 518.

/12/ J.Roth, J.Bohdansky and W.Ottenberger,Data on Low Energy Light Ion Sputtering, IPP-Report 9/26, 1979.

/13/ K.Behringer, private communication.

Table 1

Major radius	R	= 165 cm
Minor radius	a	= 4o cm
Toroidal magnetic field	B	= 22 kG
Plasma current	I_p	= 24o kA (q = 4.4)
Electron temperature	T_e	= 0.5 - 1.2 keV
Ion temperature	T_i	= 0.5 - 0.85 keV
Line averaged density	$\bar{n}_e$	= 0.2 - 6 · 1o^{13} cm^{-3}
	Z_{eff}	= 1 - 5
Energy confinement time	τ_E	$\leq$7o msec

Figure Captions

Fig. 1: Cross section of the ASDEX tokamak
1a: Divertor configuration
1b: Material limiter configuration

Fig. 2: Toroidal position of ring- and mushroom limiter, the gas input valve and the diagnostic equipment.

Fig. 3: Toroidal section of the plasma with the two movable ring limiter wings. Δr is the distance limiter-separatrix measured close to the limiter.

Fig. 4: Charge exchange spectra measured close to the limiter during several identical plasma shots with different distances Δr of the outside limiter wing to the separatrix.

Fig. 5: Time variation of the particle flux ϕ at a particle energy of 75o eV. The flux is measured close to the limiter. The limiter-separatrix distance Δr is varied between 4 and 11 cm.

Fig. 6: Variation of the normalized charge exchange flux at a particle energy of 2 keV with limiter-separatrix distance Δr. Dots are obtained close to the ring limiter; circles are obtained 45° away from the limiter. The data are normalized to 1 when the limiter is far from the separatrix.

Fig. 7: Geometry for measuring the toroidal variation of the charge exchange flux emitted close to the limiter.

Fig. 8: Charge exchange flux spectra $d\phi/dE$ measured at different toroidal distances $R\Delta\varphi$ from the ring limiter.

Fig. 9: Neutral gas density profiles $n_o(r)$ in planes with different toroidal distances $R\Delta\varphi$ from the ring limiter.

Fig.1o: Area integral $\int n_o df$ of the neutral density versus the toroidal distance $R\Delta\varphi$ from the ring limiter. The density decreases with a characteristic length of 43 cm.

Fig.11: Normalized charge exchange flux ϕ for different particle energies plotted versus the toroidal distance $R\Delta\varphi$ from the ring limiter.

Fig.12: Time variation of the external gas input $\dot{Q}_G$ to produce the plotted line density (dashed curve) for different limiter-separatrix distances Δr.

Fig.12a: The outside wing of the ring limiter is moved (the external gas input is switched off at .7 sec so that the electron density decays consecutively).

12b: The stainless steel mushroom limiter is moved.

Fig.13: Calculation of the external gas input $\dot{Q}_G$ to produce the plotted line density (dashed curve) with the assumption that the stainless steel limiter material saturates at a hydrogen fluence of $2 \cdot 10^{18}$ protons/cm^2 /9/.

Fig.14: Time variation of the line averaged density $\bar{n}$ and the charge exchange flux ϕ measured at the limiter position of a divertor (D) and a limiter (L) discharge.

Fig.15: Time variation of the external gas input $\dot{Q}_G$ to produce the plotted line density (dashed curve) for different limiter-separatrix distances Δr. The mushroom limiter material is graphite.

Fig.16: Variation of the charge exchange flux $d\phi/dE$ with the distance limiter to separatrix Δr at a particle energy of 5oo eV. The measurement is carried out at the position of the ring limiter.
Solid line: Variation of the outside limiter wing.
Dashed line: Variation of the inside limiter wing.

Fig.17: Charge exchange flux spectra $d\phi/dE$ measured with both limiter wings moved to the wall (circles) and spectra measured with the inside limiter wing rotated to the plasma (dots).

17a: The plasma is centered; the insert shows the double null divertor configuration.

17b: The plasma is shifted upward by 3 cm; the insert shows a single null divertor configuration.

Fig.18: Relation between the external gas input $\dot{Q}_G$ and the charge exchange flux ϕ measured at the limiter position for two different particle energies. $\dot{Q}_G$ and ϕ are varied together by moving the outside limiter wing to the separatrix.

Fig.19: Variation of the ohmic heating power P_{OH}, central electron temperature T_e and central ion temperature T_i with the limiter separatrix distance Δr using
a) the stainless steel wing limiter,
b) the SiC-mushroom limiter, and
c) the graphite-mushroom limiter.

Fig.2o: Variation of the central ion temperature $T_i(0)$ with the distance Δr of the outside wing of the ring limiter at different moments during the discharge.

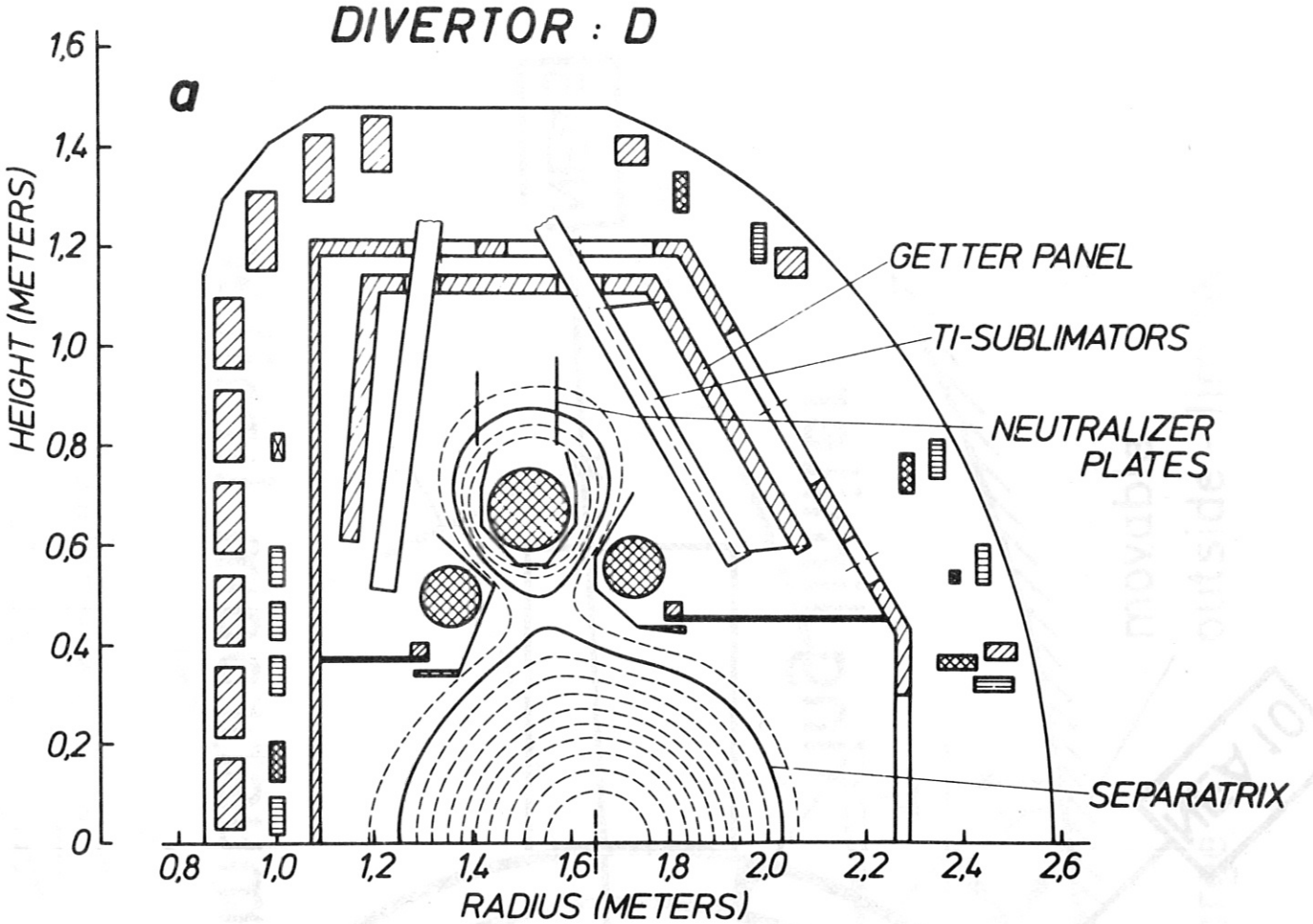
DIVERTOR : D
a
HEIGHT (METERS)
1,6
1,4
1,2
1,0
0,8
0,6
0,4
0,2
0
0,8
1,0
1,2
1,4
1,6
1,8
2,0
2,2
2,4
2,6
RADIUS (METERS)
GETTER PANEL
TI-SUBLIMATORS
NEUTRALIZER PLATES
SEPARATRIX

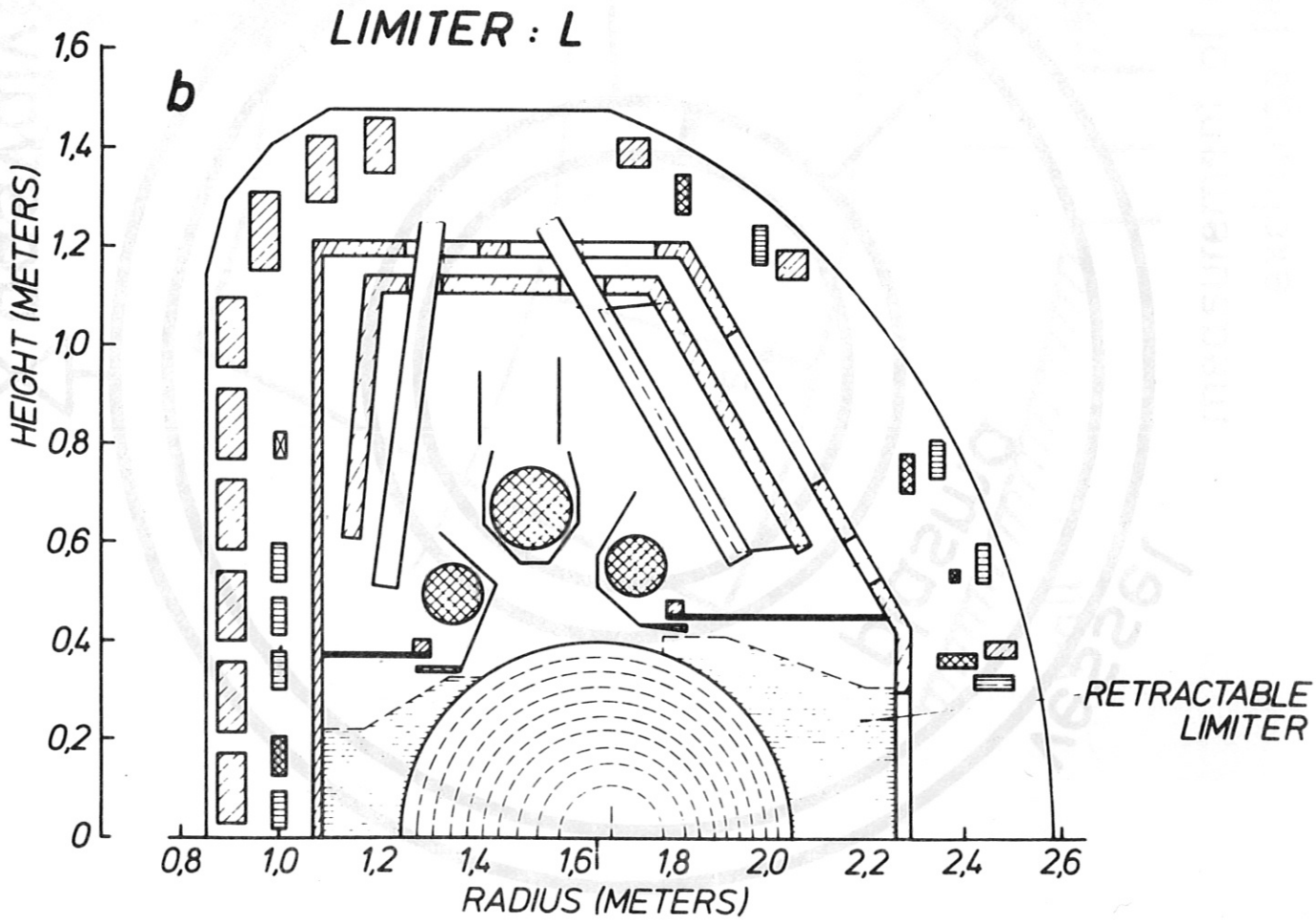
LIMITER : L
b
HEIGHT (METERS)
1,6
1,4
1,2
1,0
0,8
0,6
0,4
0,2
0
0,8
1,0
1,2
1,4
1,6
1,8
2,0
2,2
2,4
2,6
RADIUS (METERS)
RETRACTABLE LIMITER

Fig. 1

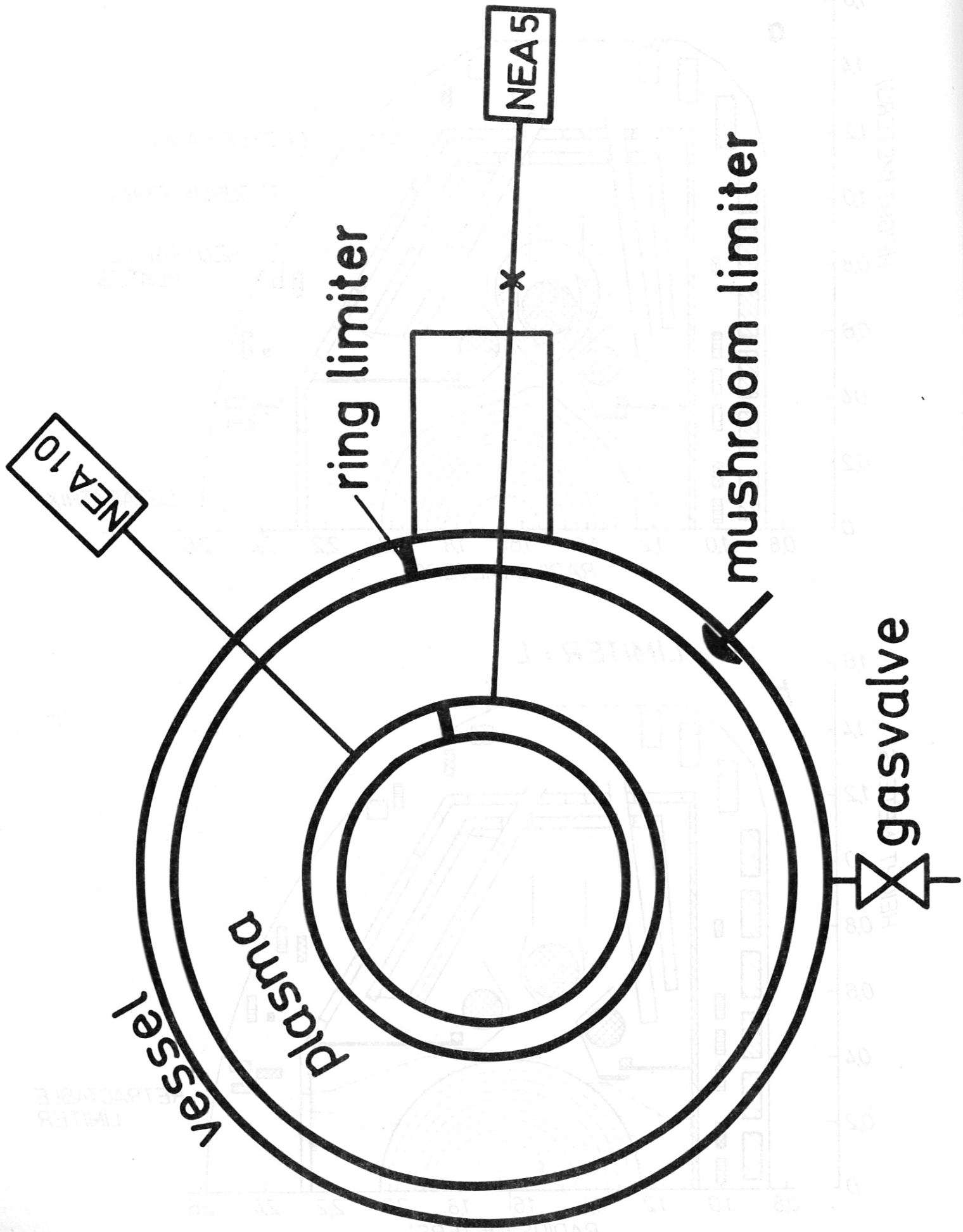
NEA 10
ring limiter
NEA 5
mushroom limiter
gasvalve
plasma
vessel

Fig. 2

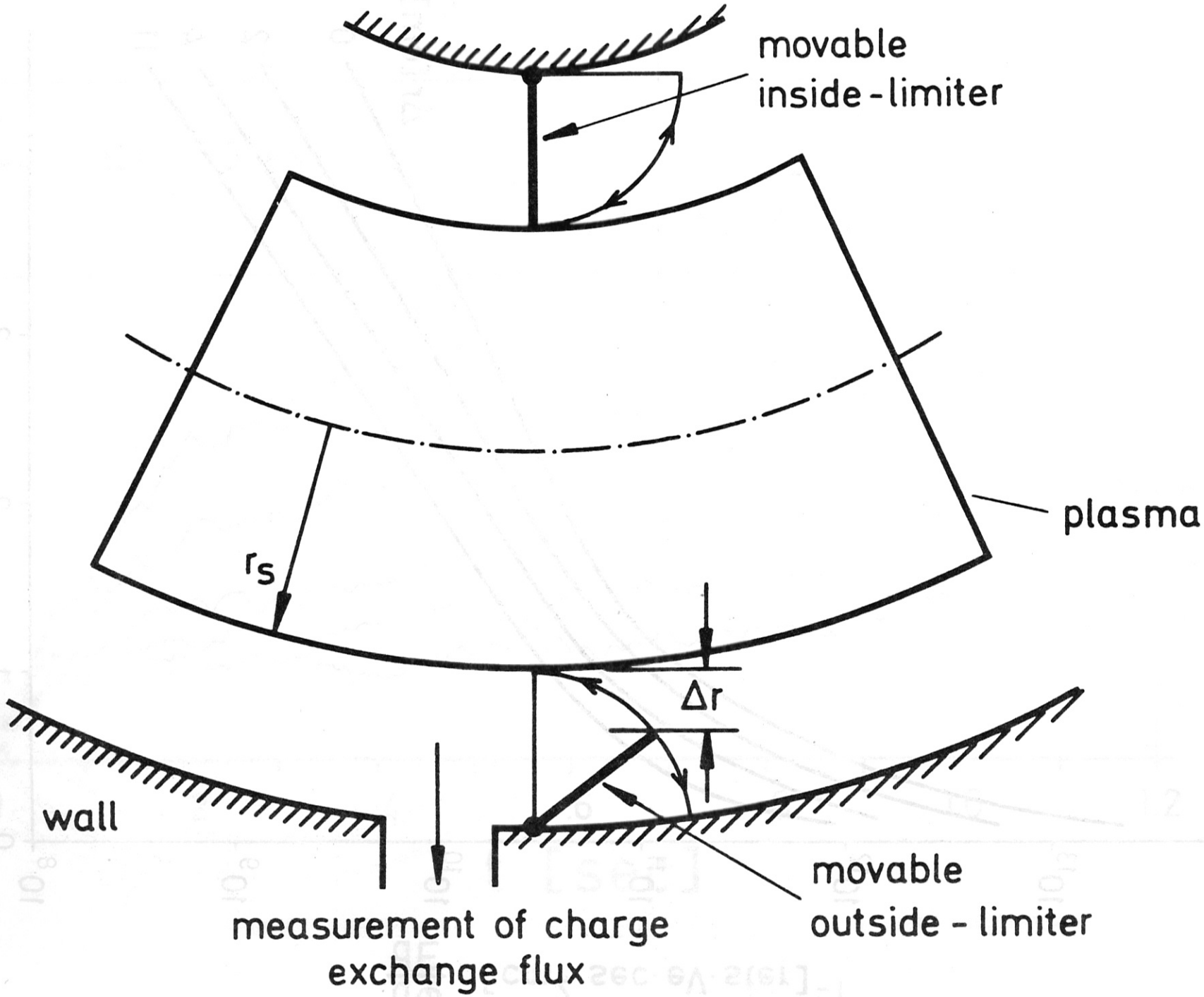
movable
inside-limiter
plasma
r_s
Δr
wall
movable
outside - limiter
measurement of charge
exchange flux

Fig. 3

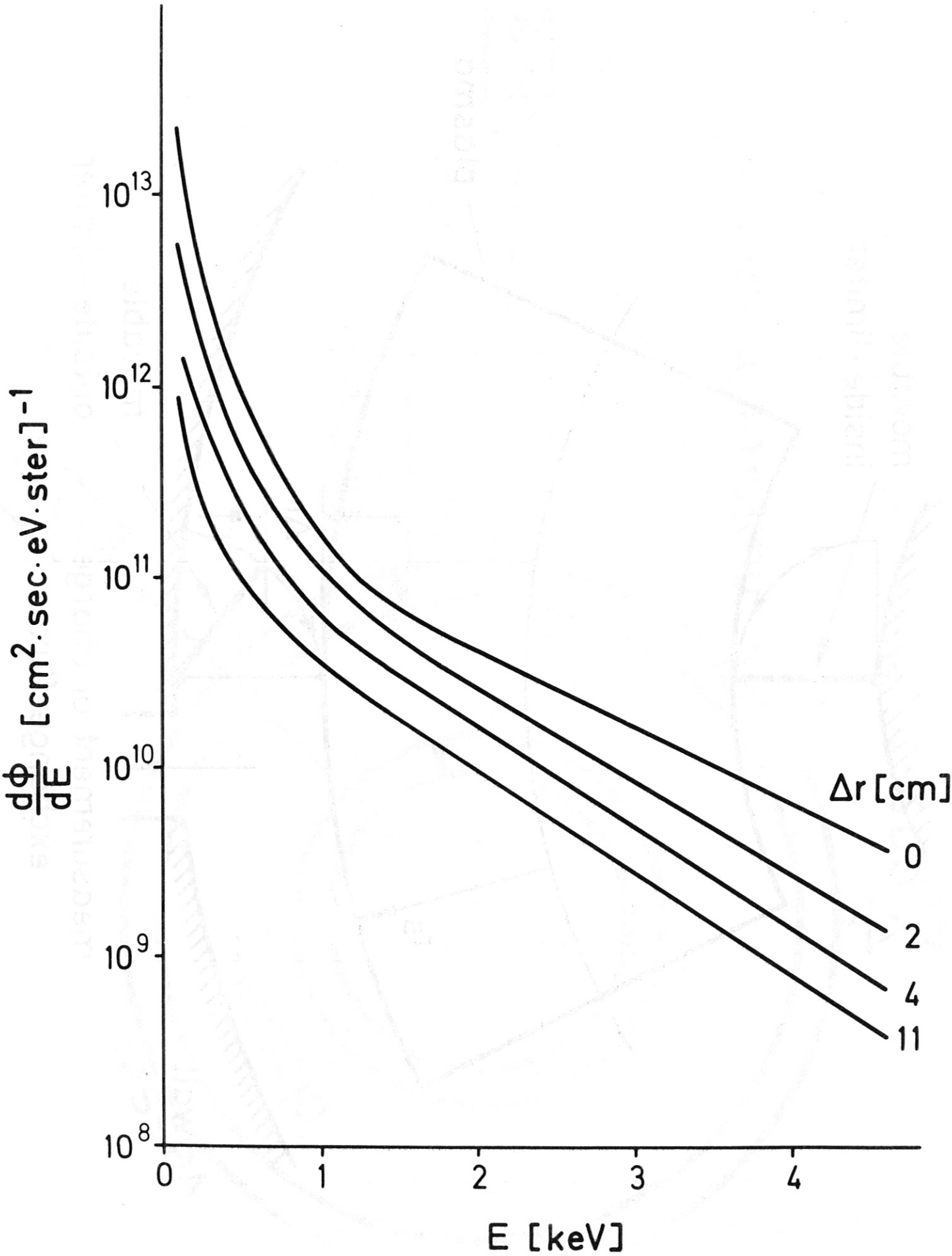
10^{13}
10^{12}
10^{11}
10^{10}
10^{9}
10^{8}
$\frac{d\Phi}{dE}$ [cm^2· sec· eV· ster]$^{-1}$
0
1
2
3
4
E [keV]
Δr [cm]
0
2
4
11

Fig.4

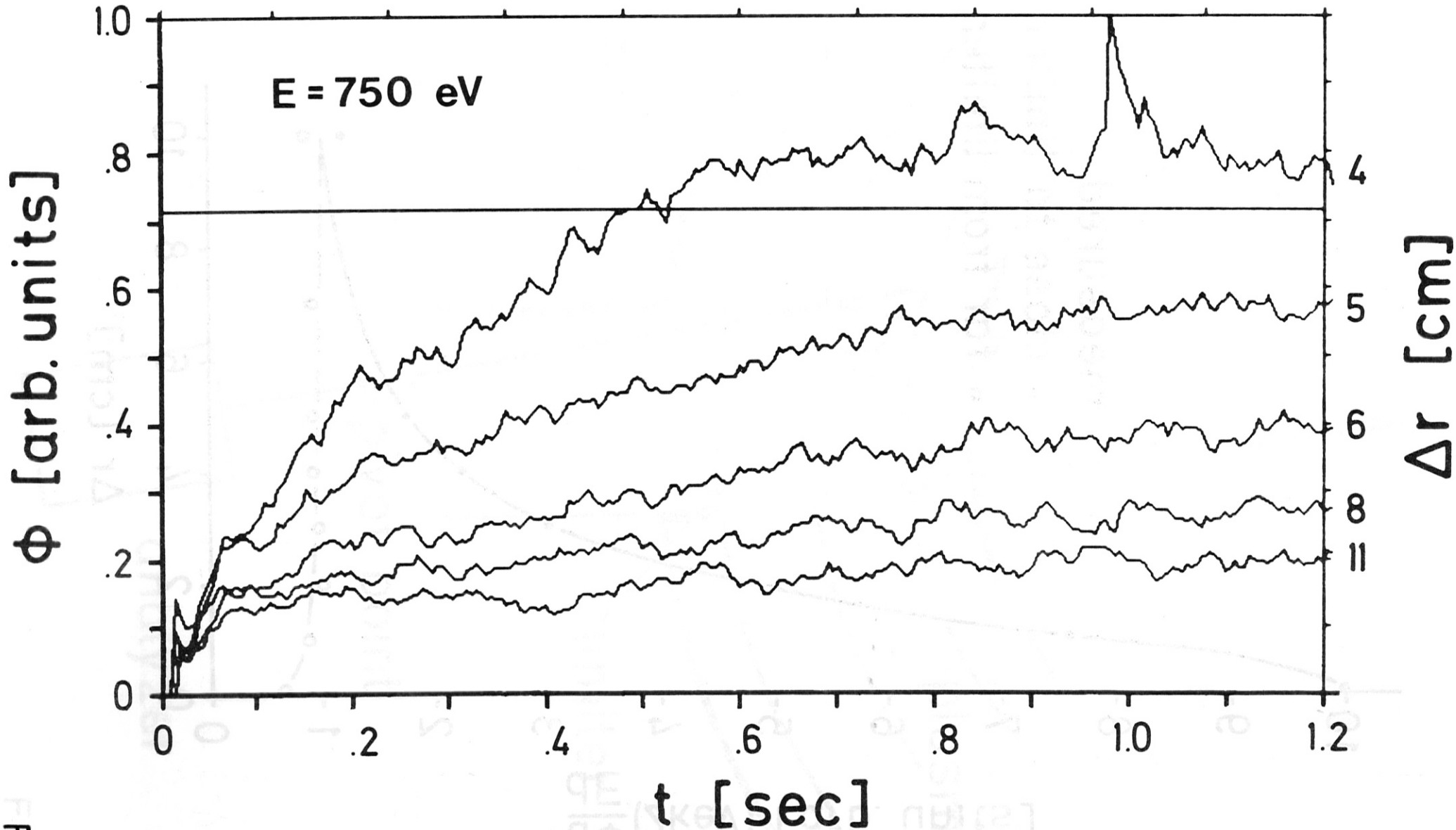

Fig.5

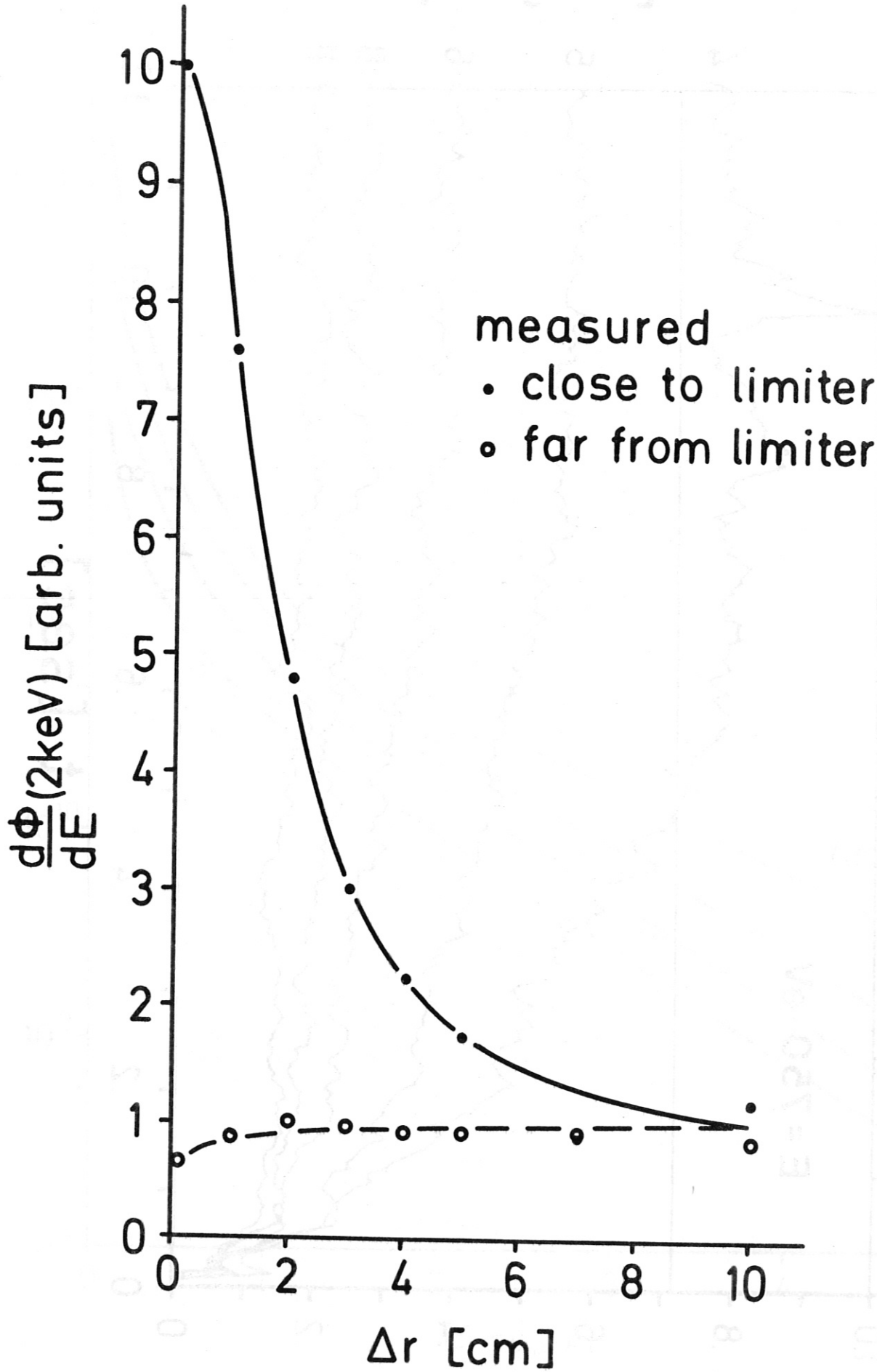
measured
• close to limiter
∘ far from limiter
$\frac{d\Phi}{dE}$(2keV) [arb. units]
Δr [cm]
0
1
2
3
4
5
6
7
8
9
10
0
2
4
6
8
10

Fig. 6

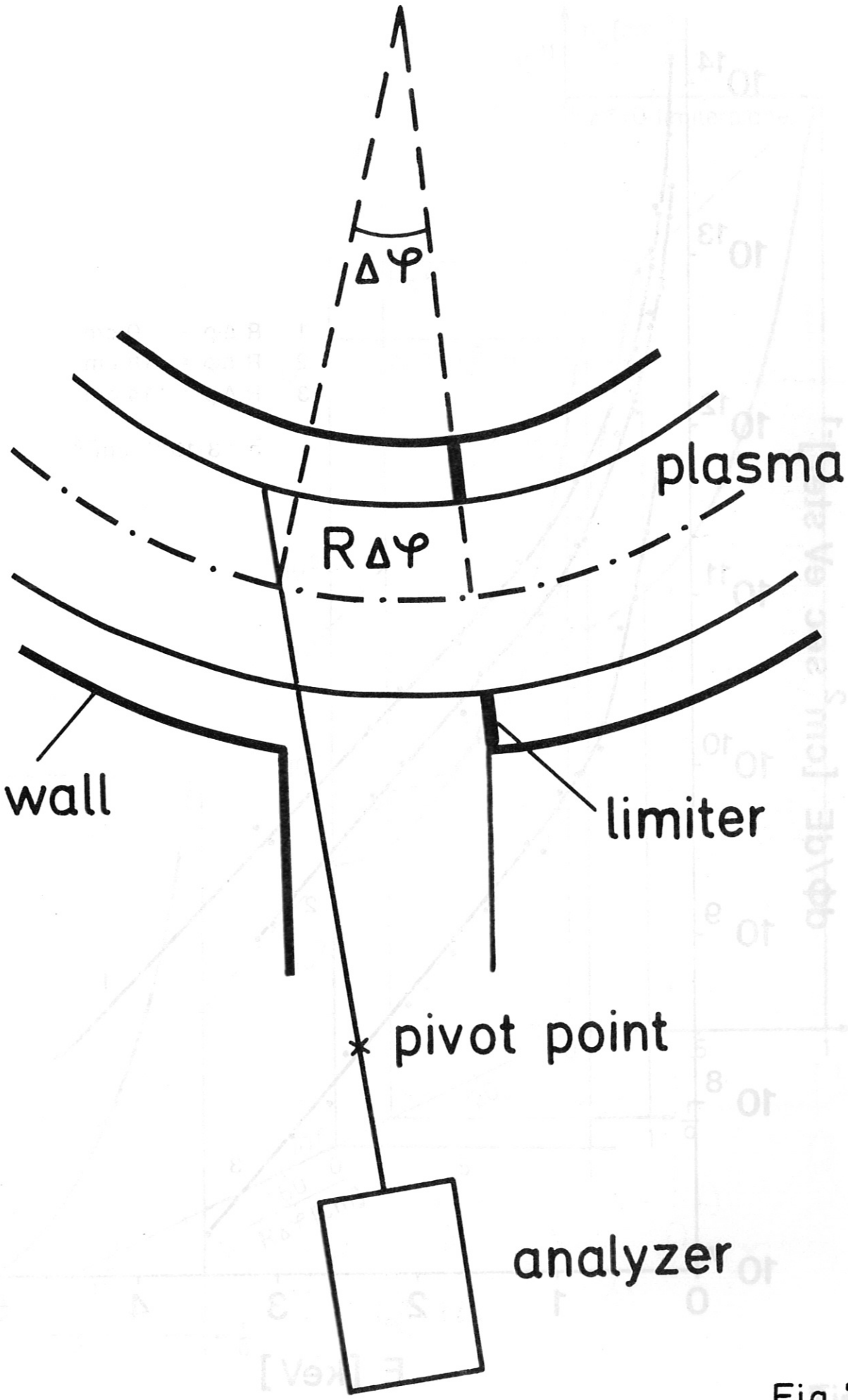

Fig. 7

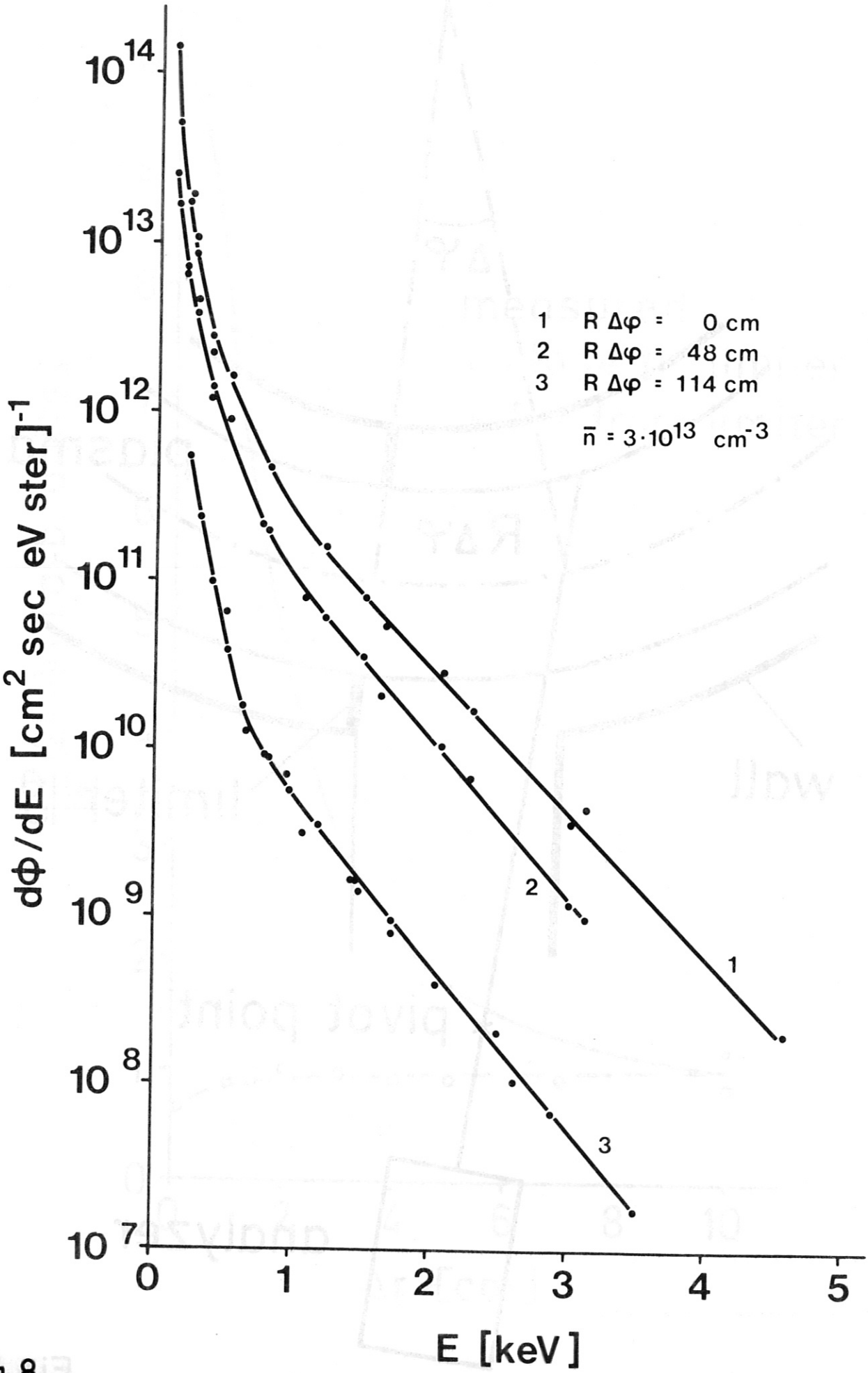
10^{14}
10^{13}
10^{12}
10^{11}
10^{10}
10^{9}
10^{8}
10^{7}
$d\Phi/dE$ [cm^2 sec eV ster]$^{-1}$
1 R Δφ = 0 cm
2 R Δφ = 48 cm
3 R Δφ = 114 cm
$\bar{n} = 3 \cdot 10^{13}$ cm^{-3}
1
2
3
0
1
2
3
4
5
E [keV]

Fig.8

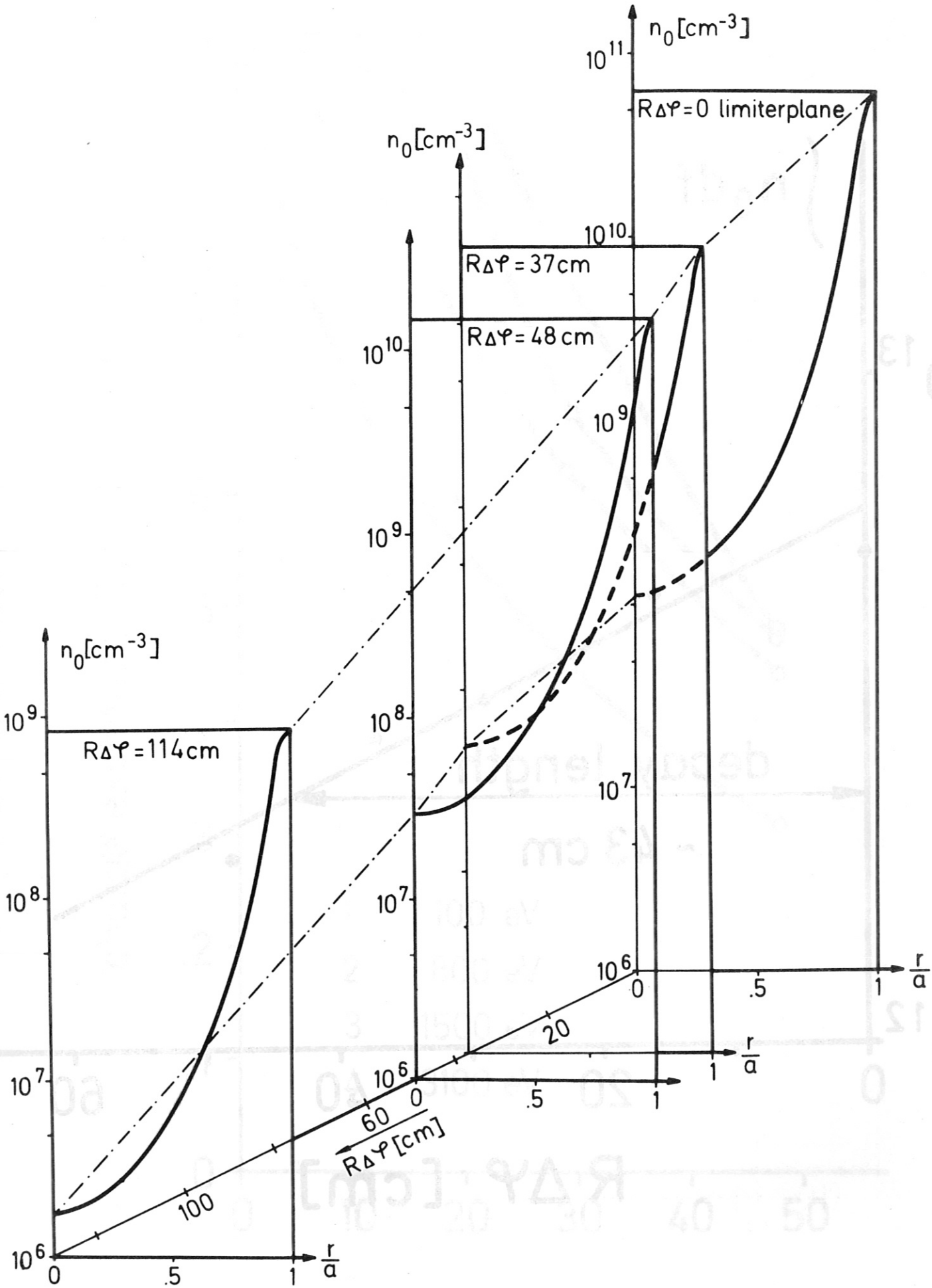
n0[cm-3]
10^11
RΔφ=0 limiterplane
10^10
RΔφ=37cm
RΔφ=48cm
10^9
10^8
10^7
10^6
RΔφ=114cm
0
.5
1
r/a
20
60
100
RΔφ[cm]

Fig. 9

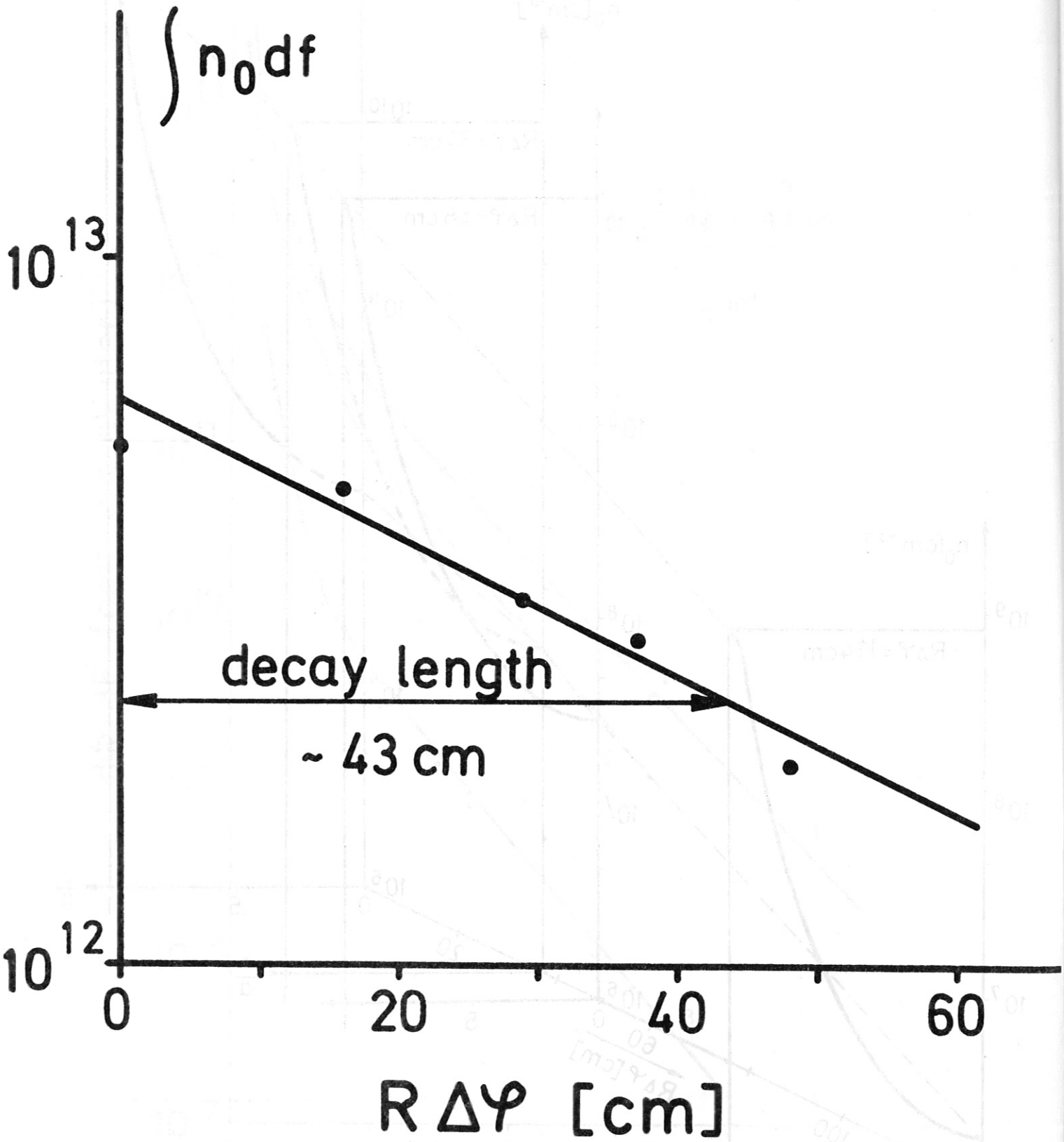
$\int n_0 df$
10^{13}
10^{12}
decay length
~ 43 cm
0
20
40
60
$R\Delta\varphi$ [cm]

Fig.10

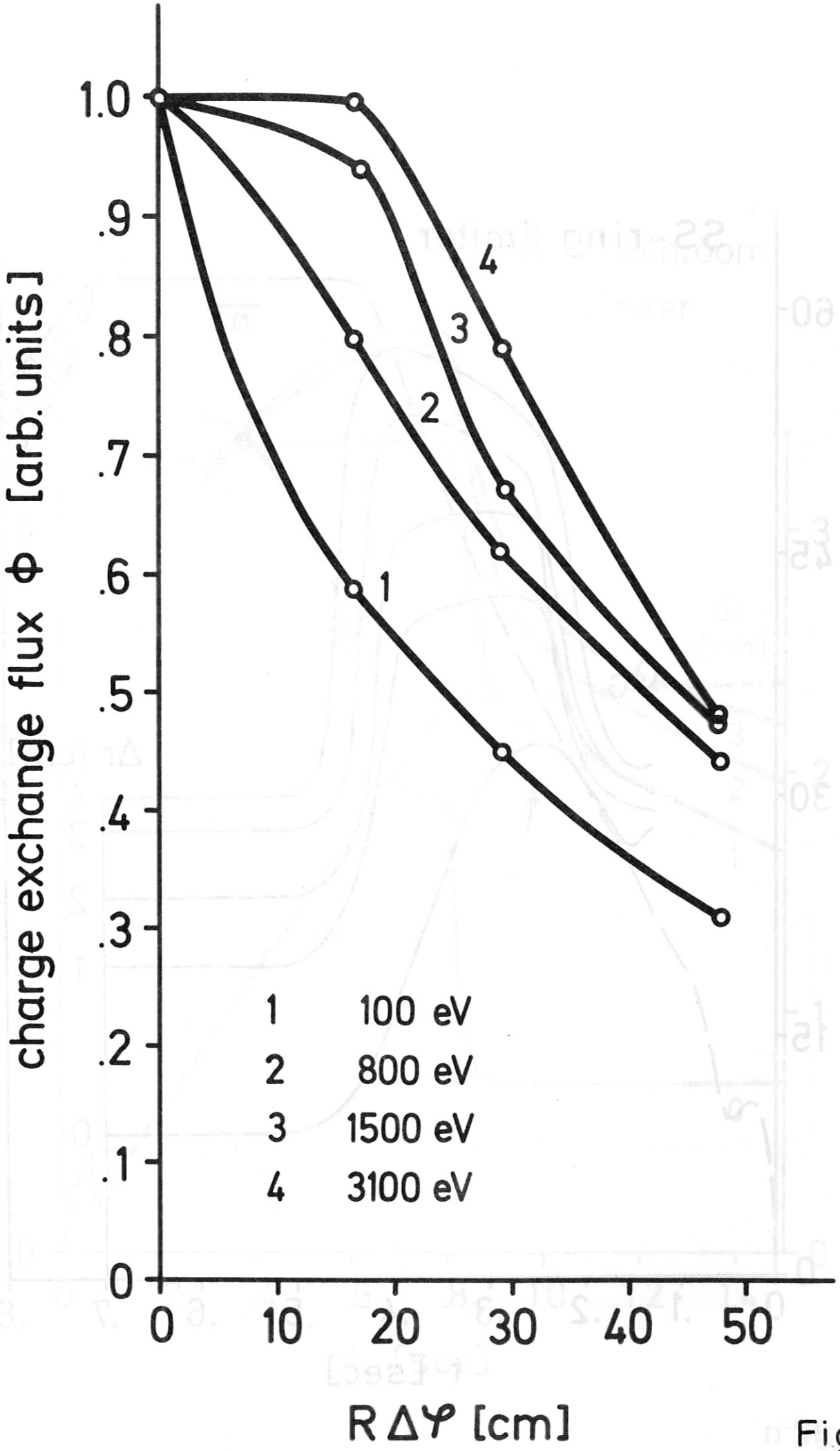
charge exchange flux Φ [arb. units]
1.0
.9
.8
.7
.6
.5
.4
.3
.2
.1
0
0
10
20
30
40
50
R Δφ [cm]
1
2
3
4
1 100 eV
2 800 eV
3 1500 eV
4 3100 eV

Fig.11

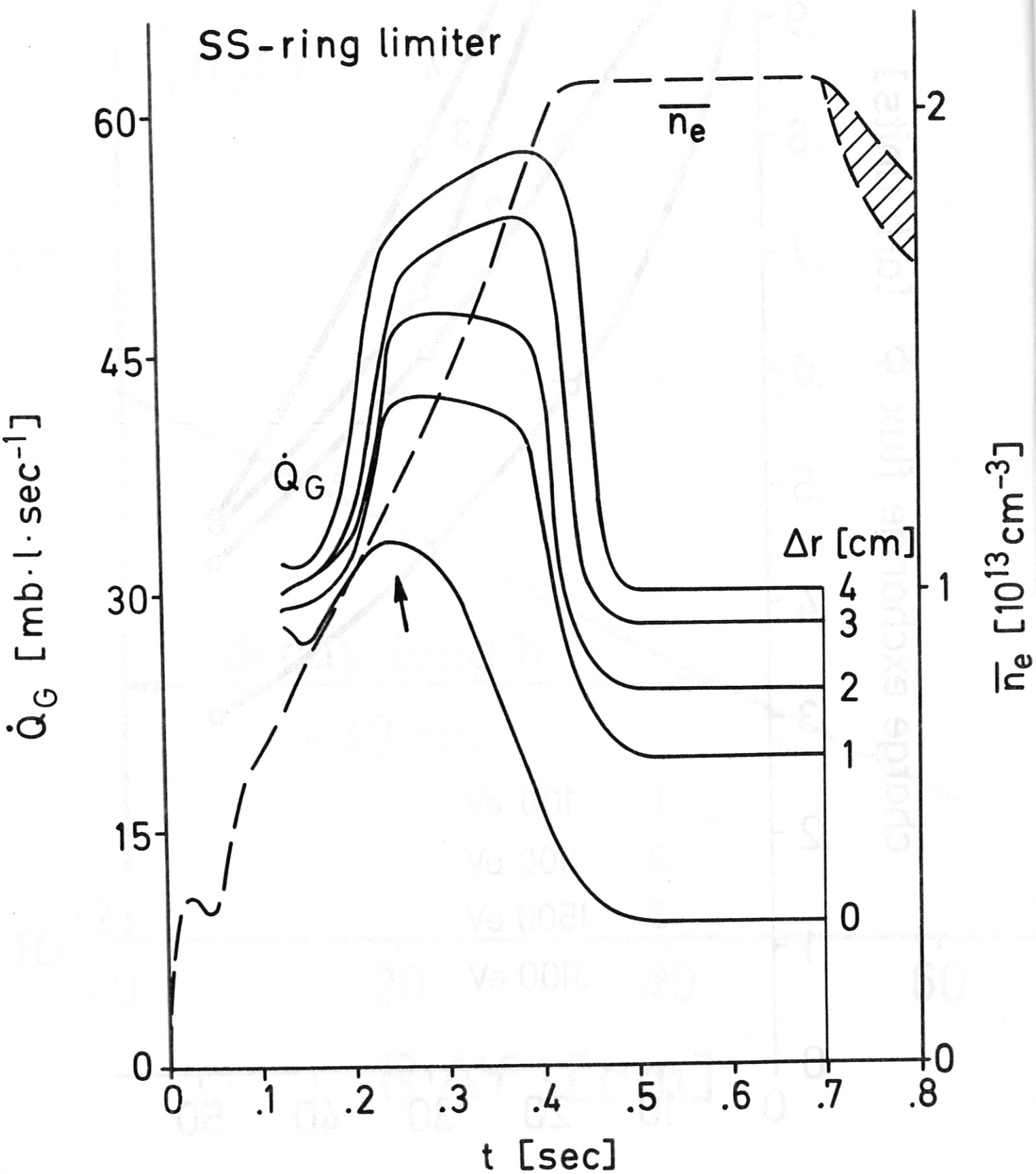
SS-ring limiter
60
45
30
15
0
$\dot{Q}_G$ [mb·l·sec^{-1}]
$\dot{Q}_G$
$\overline{n_e}$
2
1
0
$\overline{n_e}$ [10^{13}cm^{-3}]
Δr [cm]
4
3
2
1
0
0
.1
.2
.3
.4
.5
.6
.7
.8
t [sec]

Fig.12 a

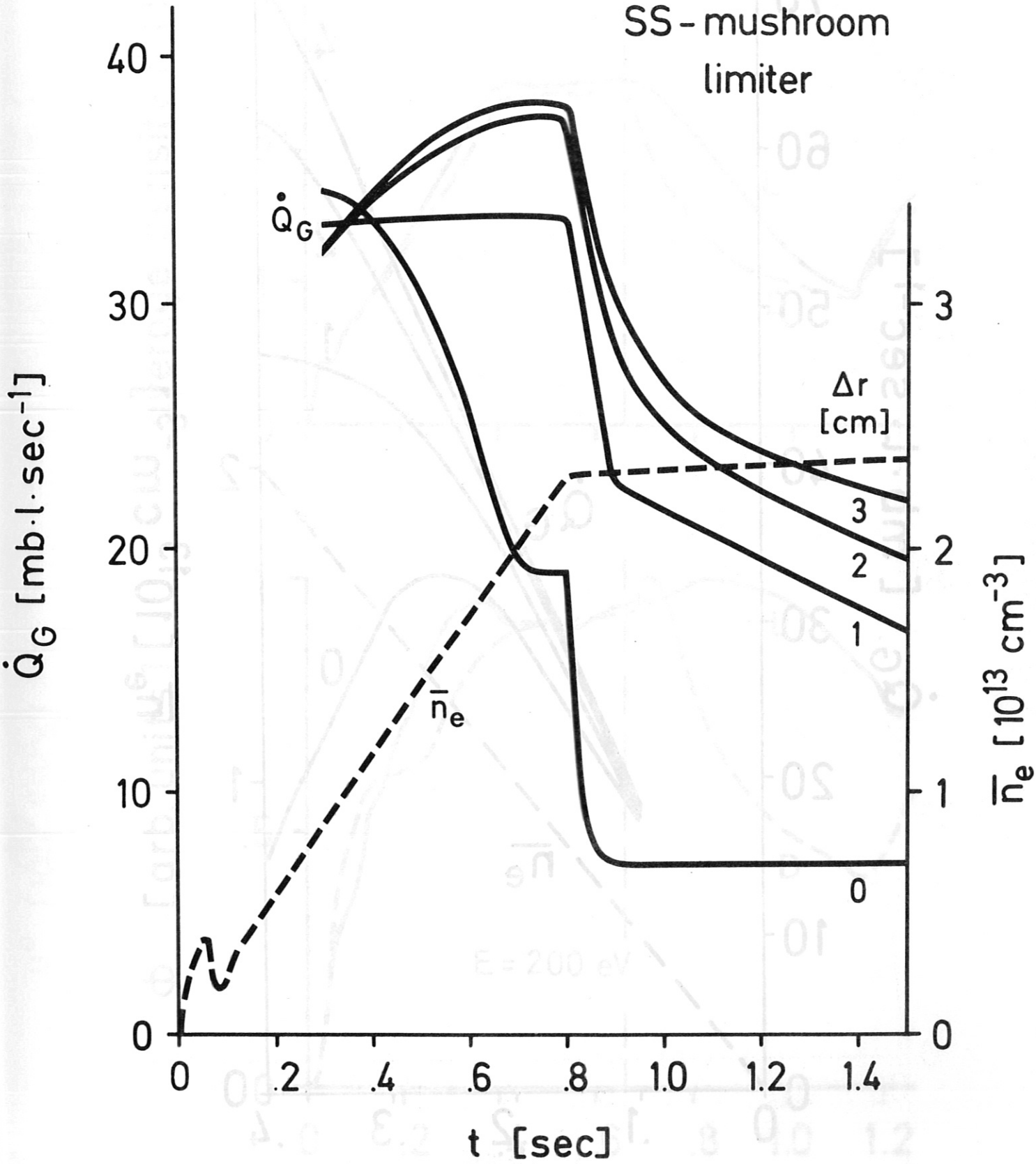
SS - mushroom
limiter
$\dot{Q}_G$
$\bar{n}_e$
Δr
[cm]
3
2
1
0
40
30
20
10
0
3
2
1
0
0
.2
.4
.6
.8
1.0
1.2
1.4
t [sec]
$\dot{Q}_G$ [mb·l·sec^{-1}]
$\bar{n}_e$ [10^{13} cm^{-3}]

Fig. 12 b

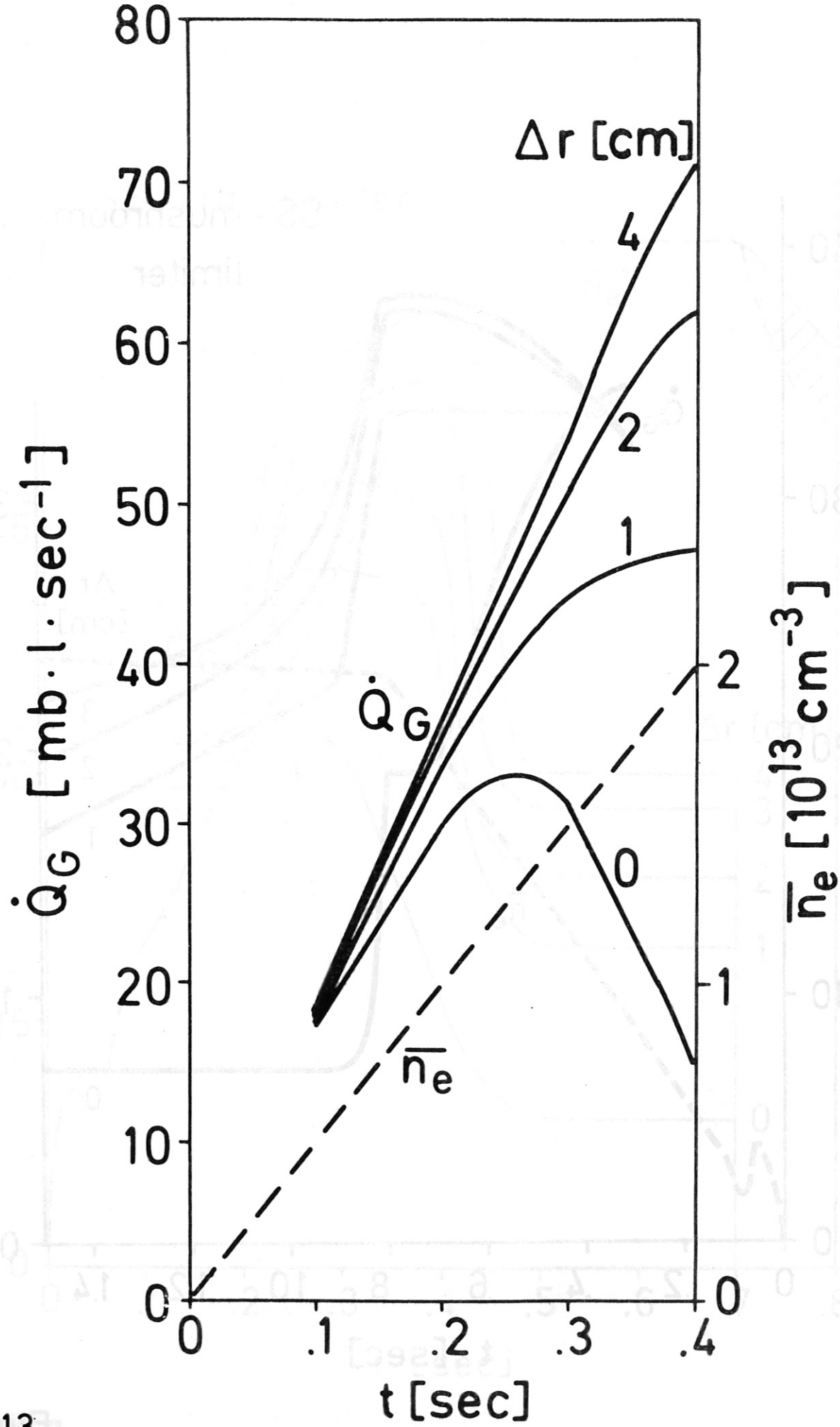
80
70
60
50
40
30
20
10
0
$\dot{Q}_G$ [mb·l·sec^{-1}]
Δr [cm]
4
2
1
0
$\dot{Q}_G$
$\overline{n_e}$
2
1
0
$\overline{n_e}$ [10^{13} cm^{-3}]
0
.1
.2
.3
.4
t [sec]

Fig. 13

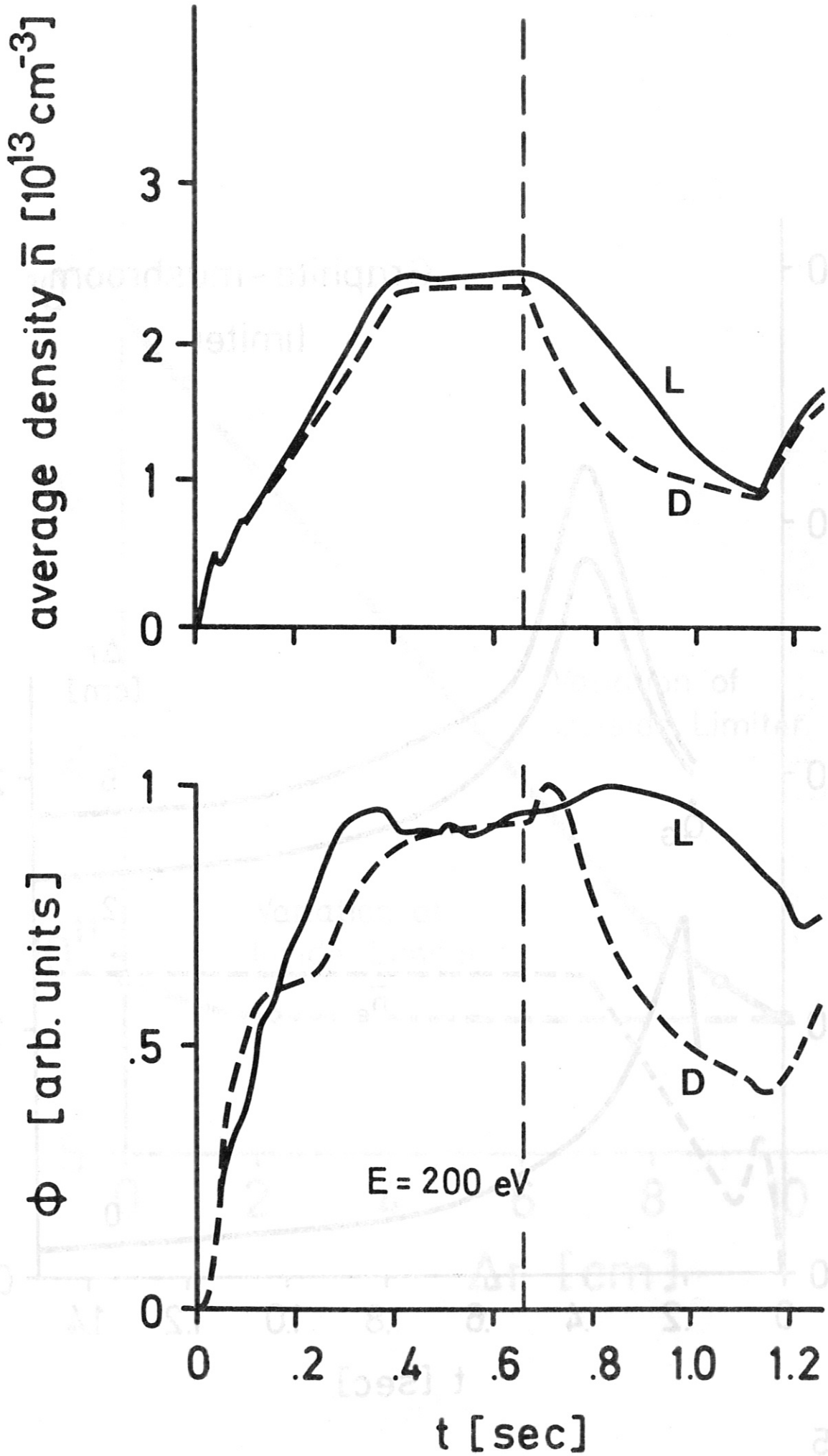
average density $\bar{n}$ [10^{13} cm^{-3}]
3
2
1
0
L
D
Φ [arb. units]
1
.5
0
L
D
E = 200 eV
0
.2
.4
.6
.8
1.0
1.2
t [sec]

Fig. 14

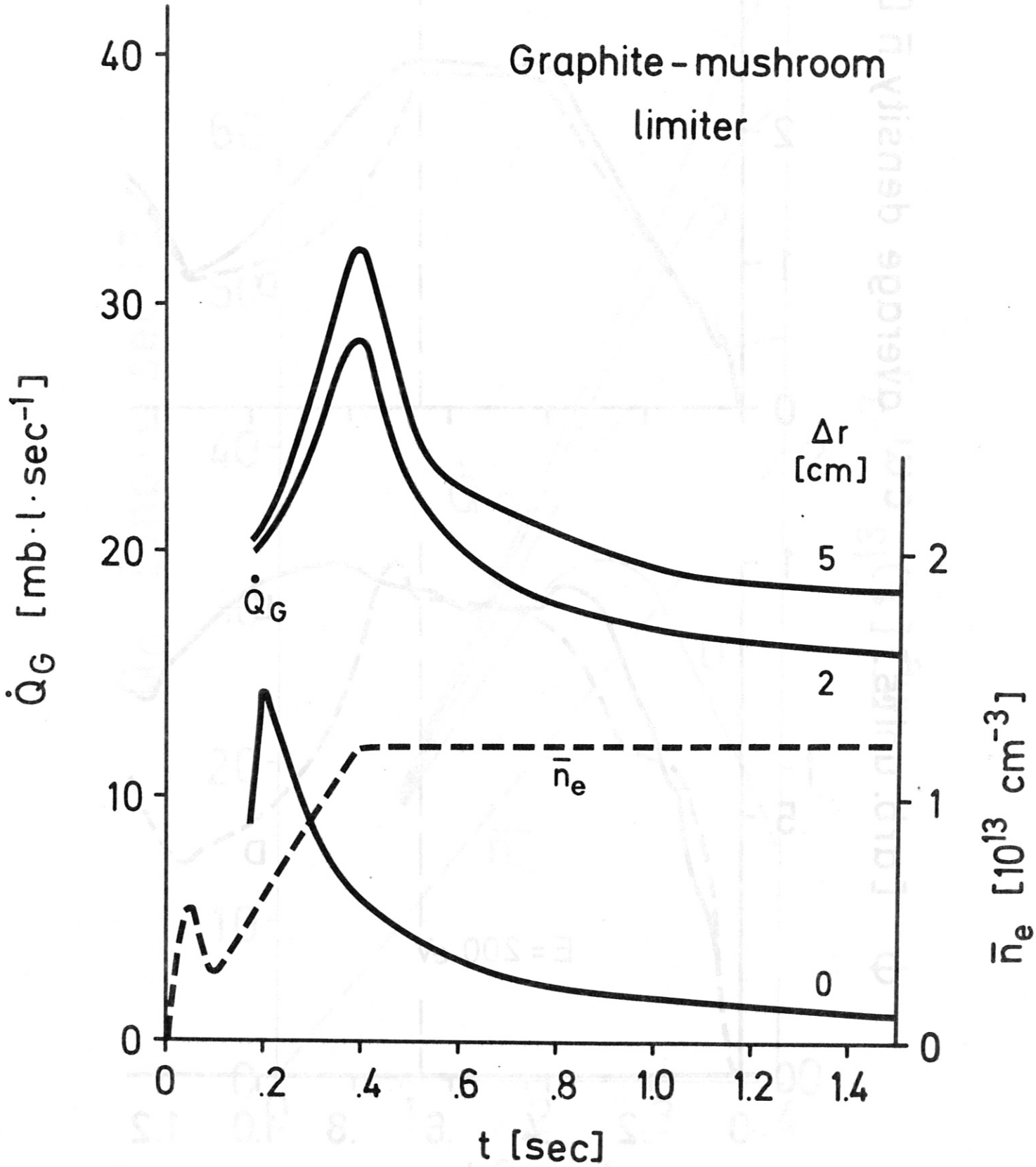
Graphite - mushroom
limiter
40
30
20
10
0
$\dot{Q}_G$ [mb·l·sec^{-1}]
$\dot{Q}_G$
Δr
[cm]
5
2
0
$\bar{n}_e$
2
1
0
$\bar{n}_e$ [10^{13} cm^{-3}]
0
.2
.4
.6
.8
1.0
1.2
1.4
t [sec]

Fig. 15

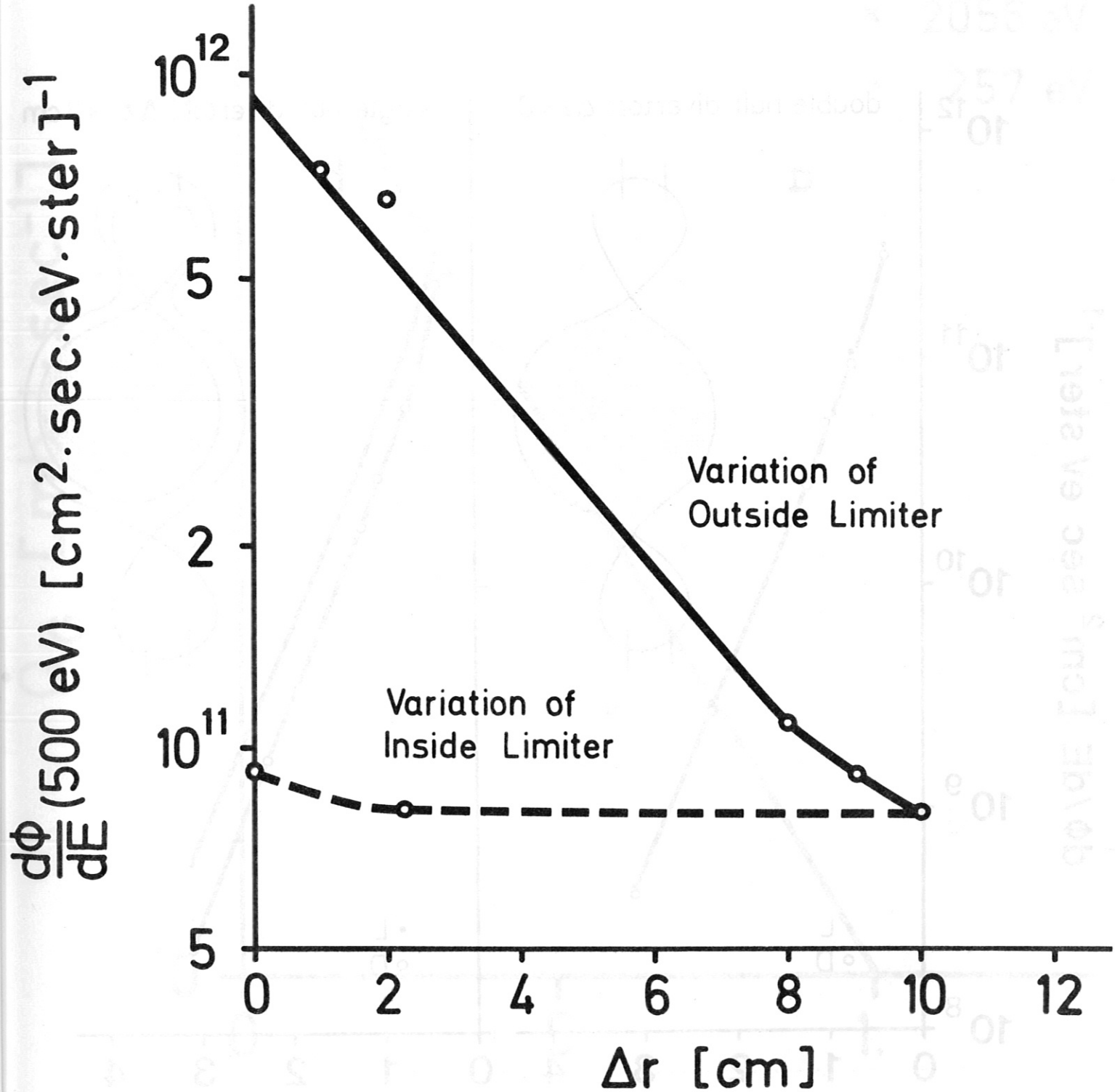
$\frac{d\Phi}{dE}$ (500 eV) [cm^2·sec·eV·ster]$^{-1}$
10^{12}
5
2
10^{11}
5
0
2
4
6
8
10
12
Δr [cm]
Variation of
Outside Limiter
Variation of
Inside Limiter

Fig. 16

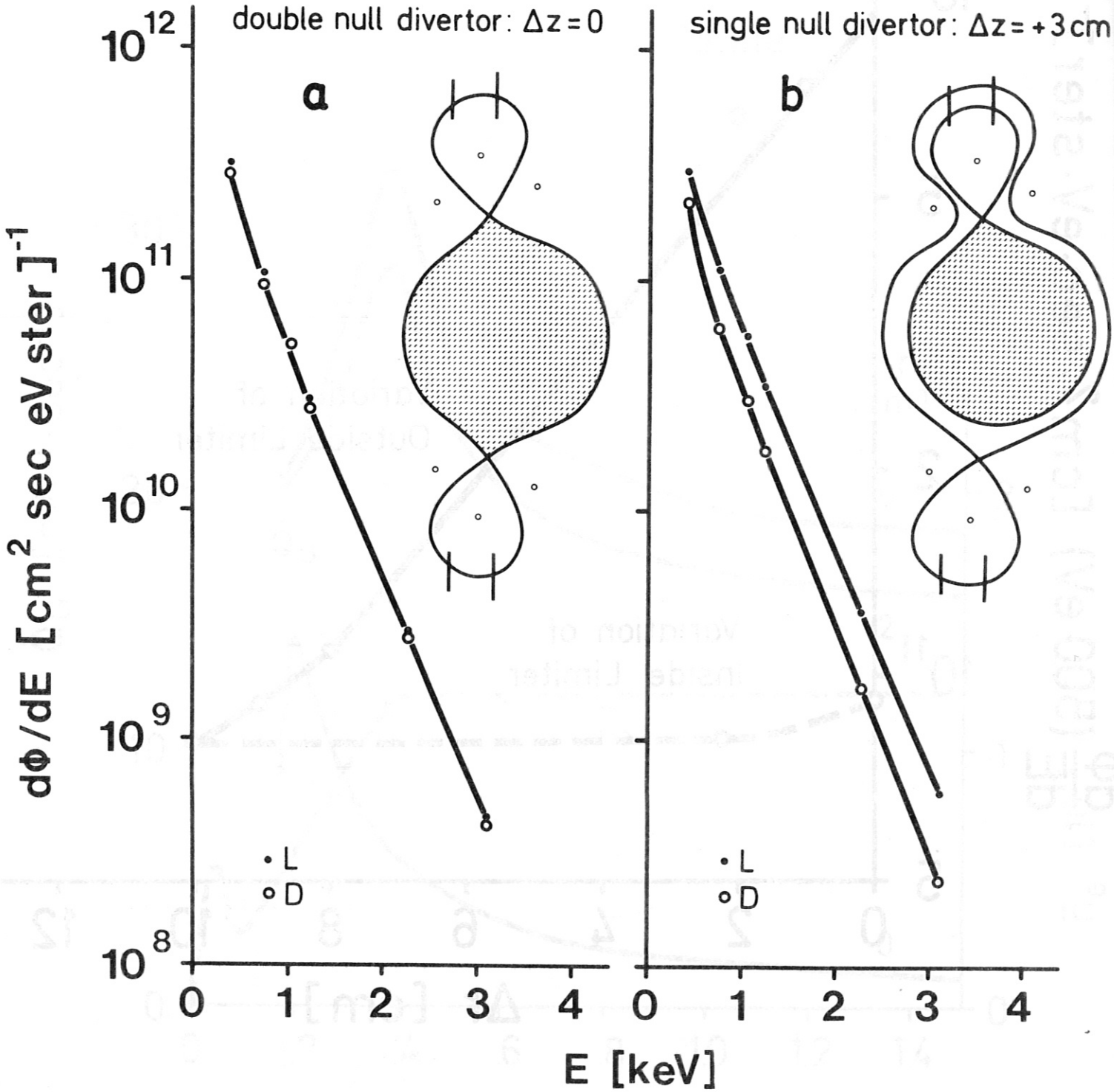
double null divertor: Δz = 0
single null divertor: Δz = +3 cm
a
b
dΦ/dE [cm² sec eV ster]⁻¹
10¹²
10¹¹
10¹⁰
10⁹
10⁸
• L
○ D
0
1
2
3
4
E [keV]

Fig. 17

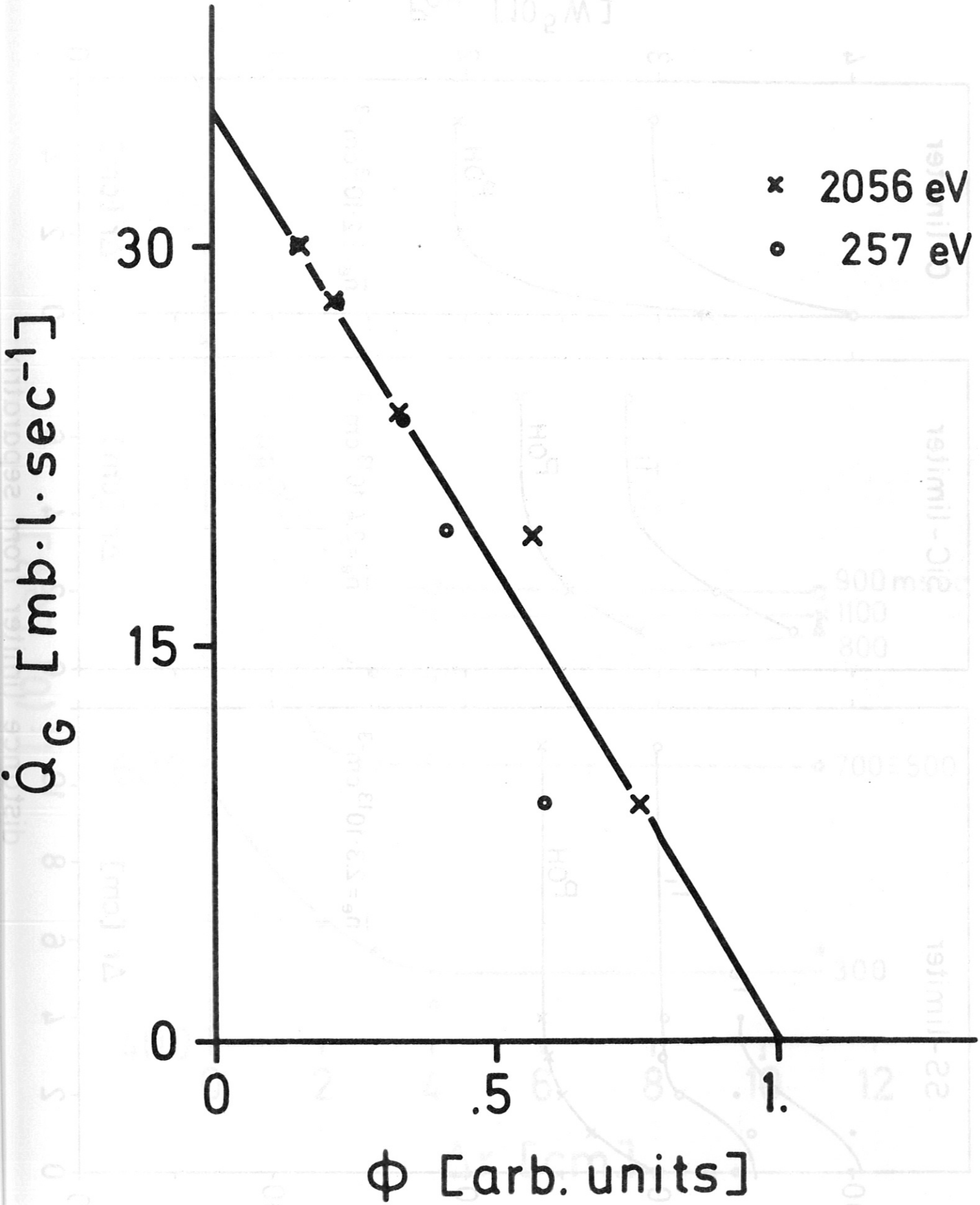

Fig. 18

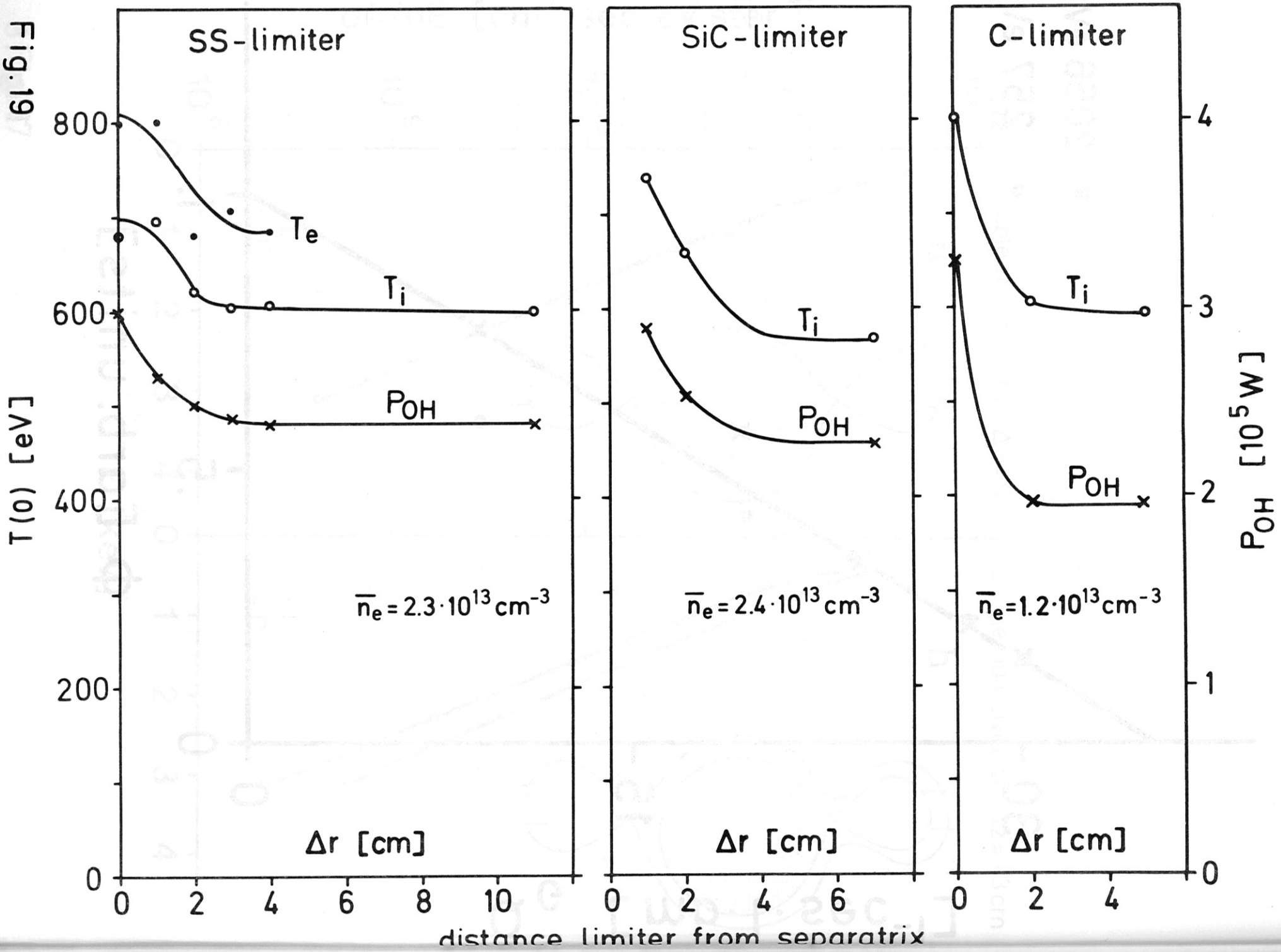
SS-limiter
SiC-limiter
C-limiter
T(0) [eV]
800
600
400
200
0
T_e
T_i
P_{OH}
$\bar{n}_e = 2.3 \cdot 10^{13}\,cm^{-3}$
$\bar{n}_e = 2.4 \cdot 10^{13}\,cm^{-3}$
$\bar{n}_e = 1.2 \cdot 10^{13}\,cm^{-3}$
Δr [cm]
0 2 4 6 8 10
0 2 4 6
0 2 4
P_{OH} [10^5 W]
4
3
2
1
0
distance limiter from separatrix

Fig. 19

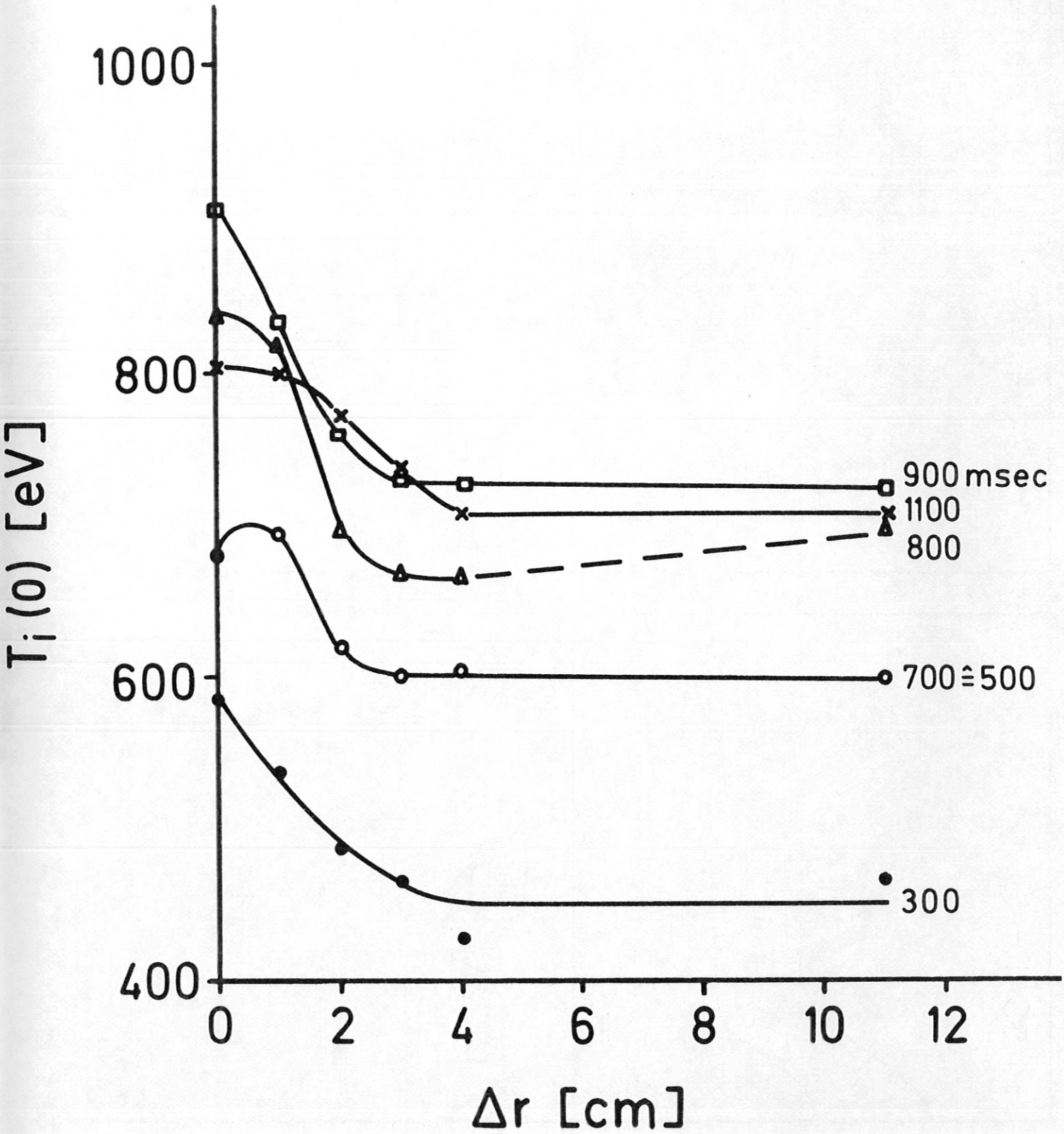
1000
800
600
400
$T_i(0)$ [eV]
0
2
4
6
8
10
12
Δr [cm]
900 msec
1100
800
700≙500
300

Fig. 20